Theor Chim Acta (1991) 80: 257–288

Theoretica Chimica Acta

Calculations of the parity non-conserving $6s \rightarrow 7s$ transition in caesium

Steven A. Blundell[1], Adam C. Hartley[2], Zuwei Liu[3], Ann-Marie Mårtensson-Pendrill[4], and J. Sapirstein[5]

[1] Department of Physics, Lawrence Livermore National Laboratory, CA 94550, USA

[2] Clarendon Laboratory, Oxford, OX1 3PU, UK

[3] Department of Physics, University of Virginia, Charlottesville, VA 22903, USA

[4] Department of Physics, Chalmers University of Technology, S-412 96 Göteborg, Sweden

[5] Department of Physics, University of Notre Dame, Notre Dame, IN 46556, USA

Received February 4, 1991/Accepted February 28, 1991

Summary. The electroweak interaction between electrons and nucleons destroys the mirror symmetry of an atom. The size of the effect depends on the weak interaction constants as well as on the atomic structure. Small-scale experiments studying atomic parity non-conservation can thus give a quantitative test of the standard model for the electro-weak interaction – provided the atomic structure is sufficiently well understood. The increasing experimental accuracy, in particular for Cs, raises new demands on atomic theory. The various contributions to the parity non-conserving electric dipole transition matrix element are discussed together with the methods used to calculate them. The uncertainty in the atomic calculation is estimated. A discussion of radiative corrections with emphasis on the role of the top quark mass is also given.

Key words: Parity nonconservation – Electronic correlation – Coupled cluster method – Relativistic many-body effects – Electroweak radiative corrections

1. Parity non-conservation

The fundamental laws of physics, as they were known until 1956, did not distinguish right from left and could never tell a physical event from its mirror image. This mirror symmetry on a fundamental level was first questioned by Purcell and Ramsey [1], who suggested that an electric dipole moment e.g. of a neutron, although violating mirror symmetry – or "parity" – could not be ruled out without experimental evidence. The year 1957 brought the discovery [2] that parity is not conserved in radioactive β-decay, leading to a rapid development of theories for the weak interaction responsible for the process. At first sight, this might not seem to have any impact on atomic or molecular physics, where the nuclear charge does not change. However, the successful *standard model* for electroweak interactions [3] predicts that the weak interaction be mediated by *intermediate vector bosons*, both a charged boson $W_{\pm}$ and a neutral boson, Z_0. The existence of weak neutral currents was demonstrated in 1973 in high-energy neutrino-nucleon scattering experiments [4]. Being as heavy as a strontium atom or a benzene molecule, these vector bosons can only mediate a very short-range interaction, leading to an increase of the effect with increasing nuclear charge. In

a pioneering paper in 1974, Bouchiat and Bouchiat [5] pointed out that the small effect of the weak neutral current interaction grows as Z^3 and could, in fact, lead to observable effects in heavy atoms. The interference of a magnetic dipole transition with a transition of electric dipole character between the same states, allowed only through the parity non-conserving weak interaction, would make even such an apparently symmetric object as an atom optically active. After an initial period of confusing and contradicting experimental results [6], the influence of weak interaction on atoms is now well established and in essential agreement with theoretical predictions. The task for atomic theory and experiment in collaboration is no longer to observe the effect but to deduce the relevant interaction constants. The calculations of parity non-conserving properties involve several subfields of physics, making it a stimulating and rewarding field, but also raising barriers. The form of the interaction and its strength depend on the model for electro-weak interaction. Some of the properties depend on the nuclear structure. The atomic calculations themselves are demanding due to the need to treat two perturbations – the external electric field, sensitive to the outer part of the electron wavefunction, and the weak interaction which takes place within the nucleus. To reach the necessary accuracy, correlation effects must be included together with relativity. The ever-increasing experimental accuracy increases the demand on atomic theory, which have stimulated the development of relativistic treatments. With sufficient accuracy, high precision tests are possible of the radiative corrections to the weak interaction theory and the advances in both theory and experiment may give a quantitative determination of the weak mixing angle θ_W, second in accuracy only to that obtained in the recent Z_0 mass determination.

The first efforts concentrated on bismuth [7–10]. Experimental as well as theoretical results have now been obtained also for the neighbouring atoms Tl [11–14] and Pb [15–17], as well as for the alkali atoms Cs [18–32, 13–14]. Today, the most accurate experimental results have been obtained for Cs, which is also the system where the atomic structure problems are least severe and in this paper we restrict ourselves to discuss the calculations for Cs. We review the methods that have been used and discuss the prospects for obtaining even higher accuracy. An accurate experiment on hydrogenic systems would of course be the joy of particle physicists, with no uncertainty related to the atomic wavefunction. However, the experiments have proven more difficult than hoped initially [33]. Recently, an experiment studying PNC in excited states of helium has been suggested [34], but no result has yet been reported. It is a challenge for us who work on calculations for many-electron systems to show that also the experiments for heavy atoms can, indeed, provide useful, reliable information.

2. Weak interactions and the atomic wavefunction

2.1. The parity non-conserving weak interaction

The weak interaction in heavy atoms is dominated by the nuclear spin-independent ("nuclear-vector electron-axial" current) part of the electron-nucleus interaction which can be written in terms of a Hamiltonian [5]:

$$h_{(1)}^{\mathrm{PNC}} = \frac{G_F}{2\sqrt{2}} Q_W \varrho_N(r) \gamma_5 . \tag{1}$$

Here $G_F = G_\mu(\hbar c)^3 = 89.6$ eV fm$^3 \approx 2.22 \times 10^{-14}$ a.u. is the weak interaction constant. The short-range character of the interaction is accounted for by $\rho_N(r)$, which is a normalized combination of the neutron and proton densities in the nucleus and is usually chosen as a Fermi distribution. The change of parity is produced by the Dirac matrix $\gamma_5 = \begin{pmatrix} 0 & 1 \\ 1 & 0 \end{pmatrix}$, which interchanges the upper and lower component of a relativistic wavefunction. The weak charge, Q_W, of the nucleus is defined as:

$$Q_W = -2[(2Z + N)C_{1u} + (Z + 2N)C_{1d}]$$

in terms of the vector coupling constants of the up and down quarks to the neutral current, given to lowest order by the "tree-level" expressions:

$$C_{1u} = -\tfrac{1}{2} + \tfrac{4}{3}\sin^2\theta_W$$
$$C_{1d} = \tfrac{1}{2} - \tfrac{2}{3}\sin^2\theta_W$$

with the weak angle θ_W related to the ratio of the vector boson masses through the relation $\cos\theta_W = M_W/M_Z$, and the present world average given by $\sin^2\theta_W = 0.226 \pm 0.005$ [35]. The values of these parameters are changed by radiative corrections [36, 37], which depend to some extent on the unknown masses of the Higgs boson and of the top quark. Earlier evaluations [36] of these corrections were based on a top quark mass of $m_t = 45$ GeV/c^2 which has now been ruled out by experiment. In addition, several definitions of $\sin^2\theta_W$ exist, which are equivalent in lowest order, but differ significantly when radiative corrections are added. Some of these aspects will be discussed in Sect. 4.4.

The Hamiltonian in Eq. (1) is derived from the current-current interaction induced by the exchange of a Z_0 boson between an electron and the nucleus. In addition to the dominating term (1) in the electron-nucleus interaction, there is one term involving the nuclear spin:

$$H^{\mathrm{PNC}}_{(2)} = -\frac{G_F}{\sqrt{2}} K_2 \varrho_N(r) \frac{(\kappa_N - 1/2)}{I(I+1)} \alpha_{\mathrm{el}} \cdot \boldsymbol{I} \tag{2}$$

where $\kappa_N = 4$ for the unpaired $g_{7/2}$ proton of ^{133}Cs and the interaction constant is $K_2 \approx -0.05$.

The weak interactions within the nucleus can lead to a helical current distribution, causing the nucleus to have an anapole moment [38, 39], defined as $\boldsymbol{a} = -\pi \int d\boldsymbol{r}\, r^2 \boldsymbol{j}(\boldsymbol{r}) = a\boldsymbol{I}$, leading to a vector potential $\boldsymbol{A}(\boldsymbol{r}) = \boldsymbol{a}\,\delta(\boldsymbol{r})$. This moment gives rise to magnetic fields inside the system but vanishes outside. The ordinary electromagnetic interaction with an anapole moment leads to a term identical in form to the spin-dependent PNC interaction in Eq. (2):

$$h^{\mathrm{PNC}}_{(a)} = \frac{G_F}{\sqrt{2}} K_a \varrho_N(r) \frac{\kappa_N}{I(I+1)} \alpha_{\mathrm{el}} \cdot \boldsymbol{I}. \tag{3}$$

Neglecting possible differences in the nuclear distribution, which have been found to have only a very small effect on the result, this interaction can be treated together with Eq. (2) by replacing K_a with $K = K_a - K_2(\kappa - 1/2)/\kappa$ in Eq. (3). As pointed out by Flambaum et al. [39] amplifying effects in the nucleus may make this interaction larger than $h^{(\mathrm{PNC}}_{(2)}$ and they estimate K to fall in the range 0.25–0.33.

Khriplovich [40] also pointed out that the combination of the nuclear spin-independent weak interaction in Eq. (1) and the ordinary hyperfine interaction

can lead to a spin dependence of the PNC transition matrix element observed.

Finally, the exchange of a Z_0 boson between the electrons leads to a two-electron interaction:

$$H_{(\text{el-el})}^{\text{PNC}} = \tfrac{1}{2}\sum_{i\neq j} h_{ij}^{\text{PNC}} = \frac{G_F}{\sqrt{32}}(1-4\sin^2\theta_W)\sum_{i\neq j}(\gamma_5^i+\gamma_5^i)(1-\alpha_i\cdot\alpha_j)\delta^3(\boldsymbol{r}_i-\boldsymbol{r}_j). \quad (4)$$

Blundell et al. [32] have calculated the effect of the electron-electron interaction in lowest order and found a contribution of the order 0.05% of the dominating effect due to the interaction in Eq. (1) [40]. The spin-dependent contributions are somewhat larger and enter at the percent level [32, 41–42]. However, by constructing a proper linear combination (depending to some extent on the calculated values for the respective transitions) of the experimental results for transitions involving different hyperfine levels, the influence of the spin-dependent part can be removed. Thus only the effect of the dominating term (1) needs to be calculated with high accuracy.

The combination of C_{1u} and C_{1d} entering for heavy atoms is essentially orthogonal to that measured in high-energy experiments [44] and, even with a precision of a few percent, the atomic PNC experiments provide some of the most stringent limits to modifications of the standard model involving extra Z bosons [36]. The particle physics implications of the restrictions on C_{1u} and C_{1d} deduced from atomic physics will be discussed in more detail in Sect. 4.4.

2.2. Observable effects

In the presence of weak interaction Hamiltonians h^{PNC} discussed in Sect. 2.1 an atomic wavefunction no longer has pure parity, but receives a small admixture of opposite parity. This makes possible an electric dipole transition from an initial state $|I\rangle$ to a state $|F\rangle$ of the same parity, where, without the PNC admixture, normally only magnetic dipole (and possibly electric quadrupole, etc.) transitions would be allowed. We note that, since the matrix elements of h^{PNC} are purely imaginary, all diagonal matrix elements of the dipole operator vanishes and h^{PNC} can thus not lead to an electric dipole moment. Only the ratio of the parity non-conserving electric dipole transition matrix element, E_1^{PNC} to another matrix element can be measured (to cancel out an arbitrary phase factor), e.g. the ratio to M_1 in the optical rotation experiments, or to the vector Stark polarizability β in the studies of h^{PNC}-Stark interference. For the accurate PNC experiments [18, 19] on Cs, β is the relevant quantity, and the calculation of β will be discussed briefly in Sect. 4.2. Most of the discussions in this paper will concern the calculation of E_1^{PNC}.

To lowest order in the weak interaction (which should be adequate, considering the smallness of G_F) the PNC electric dipole transition matrix element between an initial state I and a final state F is given by:

$$E_1^{\text{PNC}} = \sum_X \left(\frac{\langle F|\boldsymbol{D}|X\rangle\langle X|H^{\text{PNC}}|I\rangle}{E_I - E_X} + \frac{\langle F|H^{\text{PNC}}|X\rangle\langle X|\boldsymbol{D}|I\rangle}{E_F - E_X} \right) \quad (5)$$

where $\boldsymbol{D}$ is the dipole operator and the sum runs over all excited states X. In Eq. (5), I, X and F represent physical states, which can be considered as solutions to an eigenvalue equation $H|X\rangle = E_X|X\rangle$, although certain problems concerning this equation arise in the relativistic case, as discussed in Sect. 2.3. The PNC

transition matrix element can also be obtained using the PNC corrections to the wavefunctions, given to first order in the weak interaction by:

$$(E_I - H)|I^{\mathrm{PNC}}\rangle = H^{\mathrm{PNC}}|I\rangle \tag{6}$$

for the initial state, with an analogous equation for the final state F. Using these admixtures the PNC electric dipole transition element can be expressed as:

$$E_1^{\mathrm{PNC}} = \langle F|\boldsymbol{D}|I^{\mathrm{PNC}}\rangle + \langle F^{\mathrm{PNC}}|\boldsymbol{D}|I\rangle.$$

If experimental matrix elements are available, they can be inserted in Eq. (5). This is the case for the electric dipole transition elements to the first few excited states in Cs, some of which have been obtained in a critical analysis of tabulated oscillator strengths and lifetime data undertaken by the Paris group [45]. The matrix elements of H^{PNC}, on the other hand, are not directly available for experimental investigations. However, the PNC operator is closely related to the hyperfine interaction and a good estimate can be obtained by using the geometrical mean obtained on the hyperfine constants for the $s_{1/2}$ and $p_{1/2}$ states involved. This method, discussed in more detail in Sect. 3.5, has been refined by Bouchiat and Piketty [26] and its connection to many-body calculations has been analysed by Hartley and Sandars [30], who also devised methods to improve the approximation.

Equation (5) can also be evaluated with single-electron orbitals giving the first term in a many-body perturbation theory (MBPT) expansion, corresponding to the diagrams in Fig. 1. It is then, of course, necessary to consider many-body corrections. If desired, MBPT can be applied individually to the two matrix elements, as well as to the energies in the denominator of Eq. (5). This approach has been used in the most complete calculation performed to date on PNC, by Blundell et al. [32], and bridges the gap between the *ab initio* approaches and the formalism implicitly used in the semi-empirical calculations.

2.3. The relativistic Hamiltonian

For the heavy atoms used in the study of parity non-conserving effects, it is essential to use a relativistic description of the atom. A straight-forward generalization of the non-relativistic many-electron Hamiltonian is obtained by adding

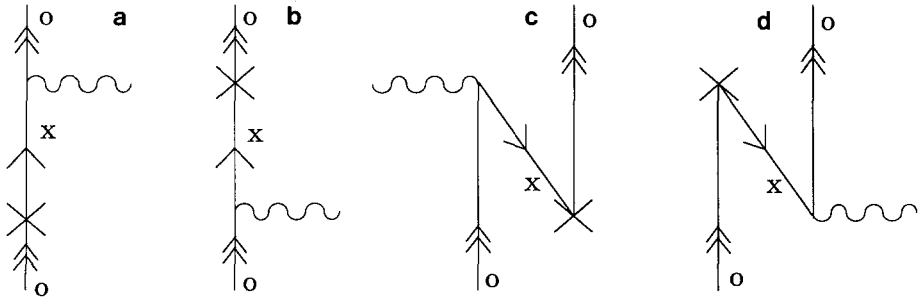

Fig. 1a–d. Diagrammatic representation of the lowest-order contributions to a parity non-conserving (PNC) electric dipole transition element. The wavy line represents the external electric field, the cross is the PNC interaction or the interaction of an electron EDM, a line with an up- (down-) going arrow represents an excited (core) orbital and a line with a double arrow represents a valence orbital

the electron-electron interaction V_{ij} to the sum of Dirac one-electron Hamiltonians, h_D, including the interaction with the nucleus:

$$H = \sum_i h_{D,i} + \sum_{i>j} V_{ij} = \sum_i (c\alpha \cdot \boldsymbol{p} + \beta mc^2 - Ze/r)_i + \sum_{i>j} V_{ij}. \tag{6}$$

However, this Hamiltonian must be treated with a considerable amount of care. Due to the existence of negative energy eigenstates to the Dirac one-electron Hamilitonian h_0, which correspond to positron states, the eigenvalue equation $H\Psi = E\Psi$, has no normalizable solutions, as first noted by Brown and Ravenhall [46] and brought back to attention by Sucher [47] – for each eigenvalue E there exists a continuous infinity of combination of one-electron states, where one electron is in the negative energy continuum and the other high in the positive one, which have a total energy E. Each two-electron state could thus dissolve into the continuum if such excitations were allowed. Of course, they are not – an excitation into a negative energy state corresponds to annihilation of a positron and can only happen when the positron has already been created (or, alternatively formulated, if an excitation out of the negative energy state has already taken place) and the creation of a virtual electron-position pair corresponds to an excitation energy of $2mc^2$. This problem arises whether the electron-electron interaction V_{12} is taken to be the pure Coulomb interaction $V_{12} = e^2/r_{12}$, or includes also the Breit interaction which accounts for the effects of virtual transverse photons. To avoid these forbidden excitations, we may surround the many-electron Hamiltonian by projection operators for positive energy states or use a second quantized formulation to ensure a proper treatment of all states. The projection operators depend to some extent on the choice of potential defining the one-electron basis. Free-electron projection operators have the advantage of mathematical simplicity in momentum space, but are quite cumbersome to work with in configuration space. Direct solution for the two-electron equation using approximate projection operators has been described by Lindroth [48] and collaborators [49]. However, given the one-electron potential, one may also choose to generate an essentially complete basis set which can be used directly in a second quantized formulation. Projection operators are then trivially implemented as a restriction of the summation. The use of a basis set consisting of known analytical functions has been discussed e.g. by Grant [50] and by Goldman and Drake [51] and this approach has been followed by Quiney et al. [52]. Discrete numerical basis sets have been used by Johnson and collaborators [27, 53], and by Salomonson and Öster [54] who expressed their basis functions in terms of piecewise polynomials and in the values on the grid points, respectively, and also by Dzuba et al. [20] who perform separate summations over the bound states and over a discretized representation of the continuum.

Most of the calculations discussed here have used the "Dirac–Hartree–Fock" (DHF, also known as "Dirac–Fock", DF) approximation as a starting point. The Hamiltonian is then divided as

$$H = \sum_i h_{0,i} + V_{\text{corr}} = \sum_i \left(c\alpha \cdot \boldsymbol{p} + \beta mc^2 - \frac{Ze}{r} + u \right)_i + \left(\tfrac{1}{2} \sum_{i \neq j} V_{ij} - \sum_i u_i \right) \tag{7}$$

where the one-electron potential u is given in the DHF case by:

$$u^{\text{DHF}} = \sum_c^{\text{occ}} \langle c | V_{12}(1 - P_{12}) | c \rangle \tag{8}$$

and the summation over occupied orbitals, c, is usually restricted to run only over the orbitals in the closed shell core, giving a spherically symmetric potential. The choice of u defines the orbital basis set and thus also the projection operators λ^+ for positive energy states. Within the no-virtual pair approximation our goal is to obtain eigenfunctions not to H but to $\Lambda^+ H \Lambda^+$, where Λ^+ assures that all electrons are in positive energy states.

The validity of the DHF approximation is sometimes questioned [47], since it is often derived from a minimization of the expectation value of Eq. (6), which has no lower in an unconstrained variation. However, in the iterative process used to obtain the DF orbitals, the projection operators are imposed implicitly through the proper boundary conditions [50] corresponding to positive energy states for each electron orbital. The DHF potential can also be derived from Brillouin's theorem, requiring the vanishing of single excitations in first order of the residual electron-electron interaction V_{corr}. This holds also for the excitation of a single virtual electron-position pair and Mittlemann [55] has found that the DHF equations can be obtained by choosing projection operators that minimize the effect of single excitations.

If the wavefunction is expressed in terms of an incomplete analytical basis set, problems may arise already at the one-particle level [56]. Cures for this "basis set disease" can be obtained by transforming the Hamiltonian to a non-relativistic form or by imposing relation between the basis for upper and lower components as reviewed, e.g. in Ref. [57].

2.4. Semi-empirical estimates

The first estimate of the PNC-E1 transition matrix element in Cs was done in the pioneering work by Bouchiat and Bouchiat [5, 58] using an elegant extension of the non-relativistic Fermi–Segrè method for hyperfine structrue combined with a relativistic correction factor (≈ 3 for Cs) which is considerably larger for the parity non-conserving weak interation than for the less singular hyperfine interaction. For the electric dipole matrix elements Bouchiat and Bouchiat used a modified Bates–Damgaard method, leading to $E_1^{\text{PNC}} = -1.33 \times 10^{-11} i|e|a_0(Q_W/-N)$.

Soon after, Loving and Sandars [59] performed a relativistic calculation using a Green's type of central potential [60] with parameters chosen to give an agreement better than 1% with the observed eigenvalues for $6s_{1/2}$, $7s_{1/2}$, $6p_{1/2}$ and $7p_{1/2}$ levels. As a natural extension of Sandars' studies [61, 62] of the closely related problem of atomic electric dipole moments, they used a single-particle approximation to Eq. (5), which is a Dirac analogue of the inhomogeneous differential equation technique introduced by Sternheimer [63]. The dipole perturbed corrections $|i^+\rangle$ and $|f^-\rangle$, respectively, to the initial and final states were obtained as solutions to the equations:

$$(\varepsilon_o \pm \omega - h_0)|o^\pm\rangle = \boldsymbol{d}|o\rangle \tag{9}$$

where $\omega = (\varepsilon_f - \varepsilon_i)$ and with the dipole operator given by $\boldsymbol{d} = e\boldsymbol{r}$ in the length form. The PNC electric dipole transition matrix element is then evaluated as:

$$E_1^{\text{PNC}} = \langle f^-|h^{\text{PNC}}|i\rangle + \langle f|h^{\text{PNC}}|i^+\rangle. \tag{10}$$

By direct insertion we see that:

$$|\sigma^{\pm}\rangle = \sum_x \frac{|x\rangle\langle x|\boldsymbol{d}|o\rangle}{\varepsilon_o \pm \omega - \varepsilon_x} \tag{11}$$

satisfies Eq. (9). We can see that Eqs. (10–11) correspond to that obtained for the diagrams in Fig. 1 from lowest order perturbation theory, using orbitals defined from the unperturbed Dirac equation. The inclusion of occupied orbitals in the summation over x in Eq. (11) may be surprising at first sight, but corresponds exactly to the diagrams in Fig. 1c,d, where the excitation of an occupied orbital into a valence state is followed by a subsequent de-excitation from a valence electron into the core hole. The sign associated with the core line in Fig. 1c,d is compensated by the opposite sign of the energy denominator obtained using ordinary diagram rules [64]. Loving and Sandars were encouraged by the good agreement between their result $E_1^{\mathrm{PNC}} = -1.15 \times 10^{-11} i|e|a_0(Q_W/-N)$ obtained in this approach and that obtained by Bouchiat and Bouchiat [58], but also emphasize that, although this "constitutes a useful check on the single-particle calculations involved" it "cannot provide evidence concerning the accuracy of the single-particle approximation itself". They also point out that "core polarization and other many-body effects make contributions of the order 10–20% in the ground state hyperfine structure of the alkalis and are likely to give appreciable effects also for the PNC-E1 transition matrix elements. However, several years passed before these effects were calculated for Cs.

The next calculation was performed by Neuffer and Commins [65] using a "Tietz" central potential [66] in the Dirac one-electron equation with the parameter chosen to give a 6*s* energy eigenvalue in agreement with experiment. They calculated explicitly the first four excited $np_{1/2}$ states in this potential and compared the sum in Eq. (5) obtained using these states to the results obtained by solving the inhomogeneous differential equation (9), which automatically gives an implicit summation over all intermediate $np_{1/2}$ one electron states in Fig. 1a,b. The effect of higher excited states was relatively small, reducing E_1^{PNC} by about 8% to $-1.00 \times 10^{-11} i|e|a_0(Q_W/-N)$. From comparison with experimental hyperfine structure they found that the p amplitude at the nucleus was about 10% low, whereas the E1 matrix elements were overestimated by a similar amount. As these effects tend to cancel, Neuffer and Commins estimate that their final result is accurate to about 10%.

In 1983, Bouchiat et al. [44] performed an extensive analysis of PNC in Cs and its implications. Their calculations were based on the Norcross semi-empirical potential in a Schrödinger equation with an added term to account for the spin-orbit interaction. Correlation factors were included to account for the effect of relativity and a finite nuclear size. They also included a semi-empirical screening in the electric dipole operator, found to give about 6% reduction of the PNC-E1 matrix element and a final result of $-0.97 \times 10^{-11} i|e|a_0(Q_W/-N)$, with an estimated uncertainty of about 10%.

2.5. Corrections to the central-field model

Already from the variations in the results obtained in various central field models, it is obvious that corrections must be applied before the results can be relied upon. These corrections can be divided into different classes, e.g. as:

(i) Corrections to the effective central potential seen by the valence electron. These corrections will include a number of high order correlation effects which may not be easy to calculate. The main advantage of the semi-empirical approaches is the ability to reproduce some of these effects, discussed in more detail in Sect. 2.6.

(ii) PNC "core polarization" in which the polarization of the core by the PNC interaction in (1) propagates to the valence electron (and to the other core electrons) via the ordinary Coulomb interaction, as illustrated in Fig. 2, below, and discussed in Sect. 2.6.

(iii) Dipolar shielding in which the core electrons respond to the external electric field, leading to a shielding of the field seen by the valence electron (Fig. 3). Like the PNC core polarization, this effect can be treated relatively easily by standard self-consistent techniques, allowing the DHF potential to include these orbital modifications, as discussed in Sect. 2.6. The shielding will also be modified by the PNC admixtures in the core orbitals (Fig. 4).

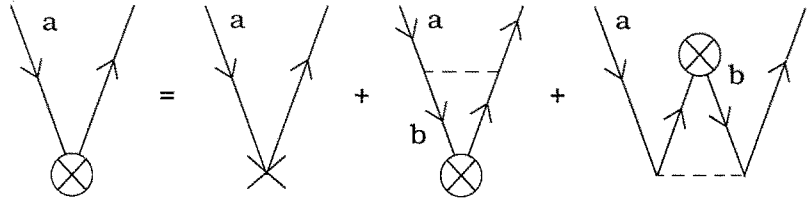

Fig. 2. Diagrammatic representation of the coupled (Dirac)–Hartree–Fock equation for a pseudo-scalar perturbation, such as the interaction with an electron EDM or the nuclear spin-independent part of weak electron-nucleus interaction

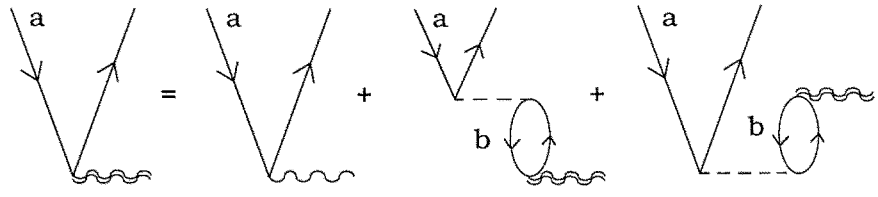

Fig. 3. Diagrammatic representation of the wavefunction modification caused by an external electric field

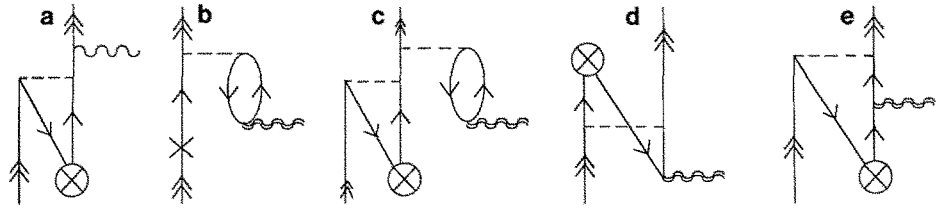

Fig. 4a–e. Examples of diagrams contributing to the total PNC electric dipole transition for a one-valence system

(iv) Complex many-body effects which are not included in (i) to (iii), above. These effects, discussed to some extent in Sect. 2.7, give contributions below the percent level for Cs, as first noted by Dzuba et al. [13].

2.6. *The Dirac–Hartree–Fock equation and additional perturbations*

In the presence of an external perturbation h, not only the valence orbital, but also all the core orbitals get perturbed. To first order in the perturbation the orbital corrections $|a^h\rangle$ satisfy the equation

$$(\varepsilon_a - h^{\mathrm{DHF}})|a^h\rangle = (h + v^h)|a\rangle - \delta\varepsilon^h|a\rangle. \tag{12}$$

The term, v^h, which was not present in Eqs. (6) or (9), is the correction to the DHF potential in Eq. (8) caused by the modification of the orbitals for the other electrons b. Keeping terms only to lowest order in the external perturbation, this potential correction is given by:

$$v^h = \sum_b^{\mathrm{core}} (\langle b|V_{12}(1-P_{12})|b^h\rangle + \langle b^h|V_{12}(1-P_{12})|b\rangle) \tag{13}$$

which is added to the RHS of (12). This leads to a set of coupled one-particle equations, which can be solved iteratively. No orthogonality has been enforced to the other occupied orbitals. The Hermiticity of the perturbation h makes $\langle b|a^h\rangle = -\langle b^h|a\rangle$ and all effects of this admixture within the core orbitals cancel, as discussed, e.g. by Heully and Mårtensson-Pendrill [67]. In general the energy correction $\delta\varepsilon^h = \langle a|h + v^h|a\rangle$ appears in Eq. (12), making the RHS orthogonal to orbital a. For odd parity operators, this term vanishes, however, as long as the unperturbed orbital $|a\rangle$ has pure parity.

Because of angular momentum restrictions, only the exchange terms enter when h is a pseudoscalar parity non-conserving interaction. A diagrammatic representation of the equations for this case is shown in Fig. 2. A frequency-dependent external electric field described by a perturbation $\boldsymbol{d}\exp i\omega t$ leads to analogous equations which, however, include the frequency dependence. The perturbation corrections $|a^{\pm}\rangle$ to orbital $|a\rangle$ are obtained from equations analogous to Eqs. (14) and (13):

$$(\varepsilon_a \pm \omega - h^{\mathrm{DHF}})|a^{\pm}\rangle = (d + v^{\pm})|a\rangle \tag{14}$$

with a frequency dependent potential correction:

$$v^{\pm} = \sum_b^{\mathrm{core}} (\langle b|V_{12}(1-P_{12})|b^{\pm}\rangle + \langle b^{\mp}|V_{12}(1-P_{12})|b\rangle). \tag{15}$$

The potential correction $v^{\pm}$ accounts for the shielding of the applied electric field and also restore the equivalence of the length and velocity forms of the dipole operator [22]. The parity conserving transition matrix element for the resonant transition $i \to f$ where $\omega = E_f - E_i \approx \varepsilon_f - \varepsilon_i$, is then evaluated as $\langle f|\boldsymbol{d} + v^+|i\rangle$. As long as the potential from the valence electron(s) is not included in $v^{\pm}$ it is not necessary to solve the equations for the frequency dependent corrections to the valence orbitals. For a frequency-dependent perturbation, the energy correction term is replaced by orthogonalization to the resonant transition so that a term $|f\rangle\langle f|\boldsymbol{d} + v^+|i\rangle$ is subtracted from the right-hand side of the equation for $|i^+\rangle$.

This powerful method of treating an additional perturbation, suggested by Sandars [68] in connection with the study of weak interactions, leads to the inclusion of several diagrams in perturbation theory at the Hartree–Fock (or DHF) level. Similar methods have been invented several times in different contexts under different names such as coupled-perturbed Hartree–Fock [69], randon-phase approximation (RPA) [70], Time-Dependent Hartree–Fock [71] and summation of single-particle excitations to all orders [72].

2.6.1. Doubly perturbed DHF orbitals. In the presence of the weak interaction or of an electron edm, all orbitals in (14) and (3–14) become parity mixed. These doubly perturbed orbitals are obtained by straight-forward generalization of Eqs. (12–15), leading to a new set of coupled equations, which we write in the more general time-dependent form analogous to Eq. (14).

$$(\varepsilon_a \pm \omega - h_0)\,|a^{\pm \mathrm{PNC}}\rangle = (d + v^{\pm})\,|a^{\mathrm{PNC}}\rangle + (h^{\mathrm{PNC}} + v^{\mathrm{PNC}})\,|a^{\pm}\rangle + v^{\pm \mathrm{PNC}}|a\rangle \tag{16}$$

where the parity-mixed frequency-dependent potential correction becomes:

$$V^{\pm \mathrm{PNC}} = \sum_{b}^{\mathrm{core}} \left(\langle b^{\mathrm{PNC}}| \frac{1}{r_{12}} (1 - P_{12})\,|b^{\pm}\rangle + \langle b^{\mp}| \frac{1}{r_{12}} (1 - P_{12})\,|b^{\mathrm{PNC}}\rangle \right.$$
$$\left. + \langle b| \frac{1}{r_{12}} (1 - P_{12})\,|b^{\pm \mathrm{PNC}}\rangle + \langle b^{\mp \mathrm{PNC}}| \frac{1}{r_{12}} (1 - P_{12})\,|b\rangle \right). \tag{17}$$

For the pseudoscalar PNC operator in Eq. (1), only exchange terms contribute. The terms on the first line are evaluated with the PNC and dipole orbital admixtures already obtained, whereas the terms on the second line change with the solutions to Eq. (16) and must be treated iteratively. Both perturbations h^{PNC} and $\boldsymbol{d}$ are odd parity operators and cannot on their own give rise to first-order energy shifts of an atomic orbital. The combination of the two perturbations, on the other hand, brings back the original parity, but since the weak interaction has purely imaginary matrix elements no energy shift arises in first order. The quantity of interest is instead the transition matrix element E_1^{PNC} which can be obtained by evaluating the overlap of the RHS of equation for $|i^{+\mathrm{PNC}}\rangle$ with $\langle f|$ giving an expression:

$$E_1^{\mathrm{PNC}} = \langle f|(d + v^{+})\,|i^{\mathrm{PNC}}\rangle + \langle f|(h^{\mathrm{PNC}} + v^{\mathrm{PNC}})\,|i^{+}\rangle + \langle f|v^{+\mathrm{PNC}}|i\rangle. \tag{18}$$

Alternatively, the overlap between $|i\rangle$ and the RHS for $\langle f^{-\mathrm{PNC}}|$ may be evaluated, giving an equivalent expression. Subtraction of $|f\rangle E_1^{\mathrm{PNC}}$ from the RHS for $|i^{+\mathrm{PNC}}\rangle$ (and of $|f\rangle (E_1^{\mathrm{PNC}})^{\dagger}$ from the RHS of the equation for $|i^{+\mathrm{PNC}}\rangle$) gives the desired orthogonalization of the resonant transition. Figure 4 shows some of the corrections to the lowest order contribution in Fig. 1.

3. Correlation effects

The coupled-perturbed Dirac–Hartree–Fock equations discussed in Sect. 2.6 often give a qualitatively correct description of a many-electron system and lead to inclusion of all many-body corrections involving only single excitations. However, correlation effects, which involve the simultaneous excitation of two or more occupied orbitals, often give effects which are of comparable importance

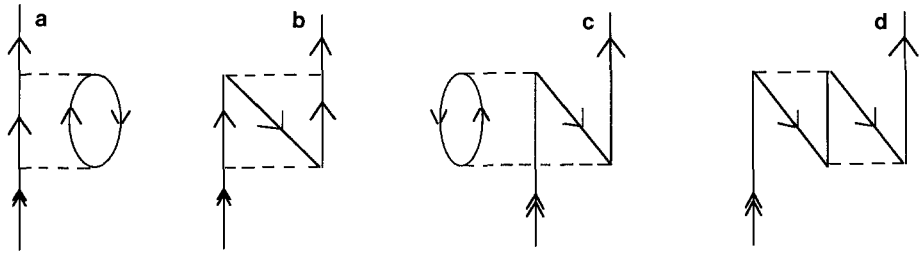

Fig. 5a–e. Diagrammatic representation of the lowest-order correlation effect on the valence orbital

and must be included in order to obtain reliable results. In this section we discuss the progress in the development of methods to include correlation effects for the problem of parity-nonconserving weak interactions in heavy atomic systems.

3.1. Correlation effects on valence orbitals

In a non-relativistic study of hyperfine structure in the alkalis, Lindgren et al. [73] noted that important correlation effects can be obtained by modifying the valence electron orbitals to approximate Brueckner orbitals. The lowest order corrections to the valence electrons are shown in Fig. 5a–d. Dzuba et al. [20] accounted for these orbital corrections by introducing a non-local correlation potential:

$$\Sigma(\varepsilon) = \sum_{s \geqslant t}^{\text{exc}} \sum_{a}^{\text{core}} \frac{\langle a|V_{12}|st\rangle\langle st|V_{12}|a\rangle}{\varepsilon + \varepsilon_a - \varepsilon_s - \varepsilon_t} - \sum_{s}^{\text{exc}} \sum_{a \geqslant b}^{\text{core}} \frac{\langle ab|V_{12}|s\rangle\langle s|V_{12}|ab\rangle}{\varepsilon_a + \varepsilon_b - \varepsilon_s - \varepsilon} \tag{20}$$

which depends, through ε, on the energy of the orbital it acts on. The lowest order correction to the orbital of the valence electron o is then given by

$$(\varepsilon_o - h_0)|\delta o\rangle = Q\Sigma(\varepsilon_o)|o\rangle = (1 - |o\rangle\langle o|)\Sigma(\varepsilon_o)|o\rangle = \Sigma(\varepsilon_o)|o\rangle - \delta\varepsilon_o|o\rangle \tag{21}$$

where the projection operator $Q = (1 - |o\rangle\langle o|)$ makes the right-hand side orthogonal to the unperturbed orbital o.

In perturbation theory the summations are often performed only over excited states, but, as the orthogonalization in Q is only performed to the orbital o itself, Eq. (21) allows admixtures of all other occupied orbitals (including negative energy states, as well as core orbitals in the relativistic case). As discussed in Sect. 2.2 these admixtures correspond to excitations from these occupied orbitals, followed by a deexcitation back into the same orbital. The extra minus sign associated with the core orbital is accounted for by an opposite sign in the energy denominator. Similarly, the energy denominator in the second term in Eq. (20) is not the one immediately expected from perturbation theory, but, as discussed in more detail in Ref. [74], it arises from a summation of terms where the next interaction occurs both before and after the second occurrence of the electron-electron interaction V_{12}.

The effect of the potential Σ in Eq. (20) acting on an open shell orbital o can be constructed in different ways. Lindgren et al. [73] in their non-relativistic work, used numerical solution of two-particle equations. However, as discussed in Sect. 2.3, due to the existence of negative energy solutions to the Dirac equation, the relativistic generalization is far from straight-forward and all relativistic applications for large atoms have instead made use of a more or less

complete basis set, keeping only the positive energy states in the summation in Eq. (20). Kelly [75] in his pioneering non-relativistic atomic perturbation theory calculations, performed the summation over intermediate states using a basis set consisting of both discrete and continuum orbitals. Dzuba et al. [13, 20, 28, 76, 77] and also Das and coworkers [12, 78] use a similar basis set in their relativistic calculations. The accuracy of an analytical basis set in the relativistic framework has been demonstrated by Quiney et al. [52]. Johnson and coworkers [53] have used B splines to construct an accurate and economical basis set, which has been applied in extensive calculations, including the study of the weak-interaction induced electric dipole transition in Cs [32]. The PNC calculations by Hartley et al. [14] were performed by using a discrete numerical basis set obtained by diagonalizing a finite-difference representation of the one-electron Hamiltonian, as described by Salomonson and Öster [54]. The different approaches give results in good agreement – provided, of course, that sufficiently large basis sets are used.

The approximate Brueckner orbital, $|o + \delta o\rangle$, constructed in this way can be used in combination with the PNC perturbed orbitals discussed in Sect. 2.7 to evaluate the lowest order correlation diagram shown in Fig. 6a (together with exchange versions, as well as Hermitian conjugate terms). Also, the potential correction v^+ can be added to account for the shielding of the external field perturbation, thereby including also diagrams such as Fig. 6d. Using electric dipole and PNC perturbed valence orbital, $|o^{\pm \mathrm{PNC}}\rangle$, it is possible to evaluate the diagrams represented by Fig. 6b. Alternatively, they may be evaluated together with corresponding diagrams in Fig. 6c by defining a parity mixed Brueckner orbital correction which satisfies the equation

$$(\varepsilon_o - h_0)|\delta o^{\mathrm{PNC}}\rangle = (h^{\mathrm{PNC}} + v^{\mathrm{PNC}})|\delta o\rangle + \Sigma(\varepsilon_o)|o^{\mathrm{PNC}}\rangle + \Sigma^{\mathrm{PNC}}(\varepsilon_o)|o\rangle - \delta\varepsilon_o|o^{\mathrm{PNC}}\rangle \tag{22}$$

and can be obtained either by solving this equation or by direct summation using a PNC mixed basis set. In the first two terms, as well as in the last term, on the right-hand side of (22), the correlation potential Σ is unaffected by the admixtures

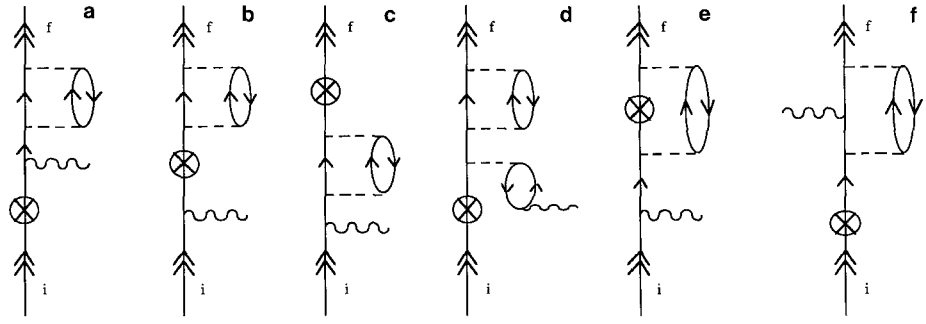

Fig. 6a–f. Examples of correlation corrections to the diagram shown in Fig. 1. The encircled cross represents h^{EDM} together with the modification, v^{EDM}, induced in the potential. Hermitian conjugate and exchange diagrams have not been shown. Diagram (**d**) is a shielding correction to diagram (**a**), similar corrections are applied to the other diagrams. Following the nomenclature by Dzuba et al. [13] the diagrams (**a–d**) are classified as "external substitutions". Diagram (**e**) is an "internal substitution" and (**f**) is a "structural radiation" term

and, following Dzuba et al. [13], these orbital corrections are referred to as "external" substitutions.

The PNC mixing may also occur in the orbitals defining the correlation potential Σ leading to a parity non-conserving part of the correlation potential $\Sigma^{\mathrm{PNC}}(\varepsilon_v)$. The parity-mixed correlation potential $\Sigma^{\mathrm{PNC}}(\varepsilon)$ is considerably more complicated and time-consuming to evaluate than the original correlation potential given in Eq. (20). Each of the terms on the right-hand side of Eq. (20) gives rise to six terms, corresponding to substitutions, both as a bra and a ket vector, of each of the three orbitals involved. Using the parity mixed correlation potential, the "internal" Brueckner orbital correction can be calculated as:

$$|\delta o_{\mathrm{int}}^{\mathrm{PNC}}\rangle = \sum_s \frac{|s\rangle\langle s|\Sigma^{\mathrm{PNC}}(\varepsilon_o)|o\rangle}{(\varepsilon_o - \varepsilon_s)}$$

and an example of such a contribution is shown in Fig. 6e. These "internal substitutions" (such as Fig. 6e) have been found to give very small contributions in the closely related case of the PNC transition in Cs [13, 27] but are significant for Tl [13].

Terms where the external field perturbation appears on an internal line in the correlation potential, giving rise to "structural radiation" corrections such as Fig. 6f, were found by Dzuba et al. [13] to be small and they ascribe the smallness of internal substitutions (Fig. 6e–f) to the double occurrence of a large energy denominator related to the excitation of a core orbital.

3.1.1. Higher-order correlation effects. From the study of parity conserving properties it is obvious that higher-order correlation effects are also necessary to obtain reliable results. A first, relatively straight-forward way to include some of the higher-order effects is to treat the correlation potential on the valence electron self-consistently, solving the equation:

$$(\varepsilon_v + \delta\varepsilon_v - h_0)|\delta v\rangle = \Sigma(\varepsilon_v)|v + \delta v\rangle - \delta\varepsilon_v|v\rangle. \tag{23}$$

This equation was solved in the early many-body calculation by Dzuba et al. [20]. Solving Eq. (23) is also one of the methods used in the recent accurate calculation by Blundell et al. [32] who found that this "chaining" of the correlation potentials significantly reduced the total correlation effects, giving results in agreement with the more complete alternative approach, discussed in Sect. 3.3.

The iteration of the correlation potential indicated in Eq. (23) corresponds to inclusion of certain terms in *even* orders of perturbation theory, but neglects, e.g. the third order diagrams shown in Fig. 7. Of these, Fig. 7b–c are among those responsible for the screening of the electron–electron interaction, emphasized by Dzuba et al. [28, 76–77] who pointed out that a lowest-order calculation of correlation effects in general gives an overestimate since this screening of the electron-electron interaction by the other electrons is not taken into account. Dzuba et al. summed these diagrams (together with analogous higher order terms) by using Feynman propagators. The relation between this approach and MBPT is analysed in Ref. 79. Another method to include higher-order correlation effects would be to solve the pair equation iteratively [80–83]. Direct application of many-body perturbation theory in its conventional intermediate normalization formulation [64] would lead to inclusion of the diagrams in Fig. 7(a–b), whereas Fig. 7(c–e) would be omitted. They could be included in a

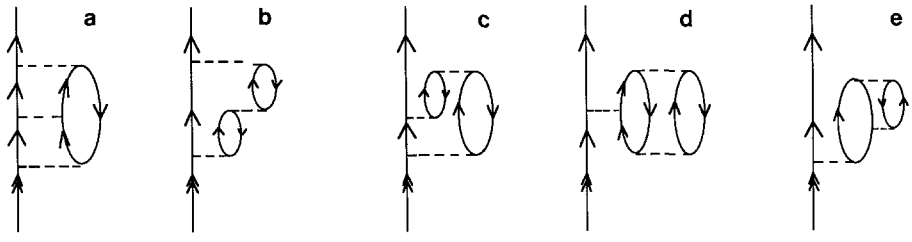

Fig. 7a–e. Examples of third-order correlation diagrams (**a–b**) would be included in an iterative solution of the pair equation. In a Hermitian formulation also (**c–e**) would be included. Diagrams (**b–c**) account for the screening of the Coulomb interaction. Diagram (**e**) could be included by including Brueckner-type correction in the occupied orbitals, if care is taken to avoid double-counting

Hermitian formulation of MBPT, as suggested, e.g. by Lindgren [84]. Recently, Blundell et al. [79] have investigated all individual third-order contributions to the binding energy Cs and Tl. They found that the screening diagrams (analogous to Fig. 7b–c) do, indeed, dominate for Cs, although contributions at the percent level arise also from other diagrams. For Tl, the importance of the remaining diagram is significantly larger.

In Sect. 3.2 we discuss the application of all-order methods within the coupled-cluster approach which has been the theme of this workshop.

3.2. The coupled-cluster approach

The coupled-cluster approach was introduced in nuclear physics by Coester and Kümmel [85–86] and in quantum chemistry by Cizek [87] and delightful presentations of its early developments were given at this workshop [88]. This approach provides a systematic way to include large classes of higher-order terms. A wave operator $\Omega = \{\exp(S)\}$ in normal ordered exponential form is then used to express the exact wavefunction Ψ terms of Ψ_0, which is an eigenfunction to the approximate Hamiltonian H_0:

$$|\Psi\rangle = \Omega|\Psi_0\rangle = \{\exp(S)\}|\Psi_0\rangle.$$

The cluster operator $S = S_1 + S_2 + S_3 + \cdots$ is the connected one-, two-, three-, ... body part of the wave operator and can be obtained from the equation:

$$[S, H_0] = (V\Omega - \Omega V_{\text{eff}})_{\text{conn}}. \tag{24}$$

The effective potential V_{eff} in Eq. (24) is added to the approximate Hamiltonian H_0 to give the effective Hamiltonian H_{eff} which has the property that it reproduces the exact eigenvalues when acting on the approximate wavefunctions. Commonly the equation for the cluster operator is derived using intermediate normalization [see e.g. Ref. 64] where $V_{\text{eff}} = PV\Omega P$. In the case where the model space defined by P includes only one state, V_{eff} gives the energy correction for this state.

The exponential Ansatz for the wave operator leads to a large number of terms on the right-hand side of Eq. (24), limited however, by the two-body character of V which makes it possible to connect at most four cluster operators in $V\Omega$. The treatment of *all* powers of the one-body cluster operator S_1 can be

trivially implemented by replacing all ket vectors $|c\rangle$ for occupied orbitals by the modified orbital $|c+\delta c\rangle$, while leaving the bra vector unchanged[1] as $\langle c|$. This approach was used e.g. in the program for complete atomic CCSD (coupled-cluster with singles and doubles) calculations developed by Salomonson and Öster [54], so far applied to Be [81, 89], Li [90], Na [91] and K [92].

Terms involving higher than the second powers of S_2 cannot lead to two-particle contributions on the right-hand side of Eq. (24), but also the inclusion of S_2^2, becomes complicated. Whereas some of the terms "factorize with respect to pair energies" and can be easily implemented essentially as energy corrections, some are quite demanding computationally. An encouraging lesson we learnt at this workshop is that the "approximate coupled pair" (ACP) approach which includes only these "hole-pair factorizable" diagrams in fact "provides results which are usually better than the full CCD approach" [93]. Paldus et al. [94] explained this observation by noting that a certain amount of cancellation exists between the contributions from true quadruple excitation clusters S_4 and the remaining S_2^2 terms.

The higher-order correlation calculations for heavy atoms is hampered by the magnitude of computational demands. In a relativistic central-field model, Cs has 17 core orbitals. Including all combinations of two-electron orbitals leads – literally – to thousands of pair excitations already when modest angular excitations are allowed. In the most complete coupled-cluster calculation performed for Cs [32, 82] Blundell et al. performed iterations for all these excitations, within a fully relativistic framework. Of the non-linear terms only the "backward diagrams" which account for the energy correction of the valence electron were included and in their first coupled-cluster calculation, which was performed for Li and Be^+ [81], they solved in effect the equation

$$[S, H_0] = (V(1+S) - SPVS)_{\text{conn}}$$

for single and double excitations

Whether or not the non-linear terms are included, the restriction to single and double excitations in S leads to neglect of the terms, such as those shown in Fig. 7c–e, where an intermediate level involves a triple excitation. Due to factorization, these terms, in fact, require only two-particle clusters and could be included ad hoc by observing that they are proper allowed terms in the conventional expansion. A more formal way of including these additional terms is provided by the Hermitian or unitary coupled-cluster approach [84, 95–96]. Lindgren used the normalization condition of Jørgensen [97] $P\Omega^\dagger\Omega P = P$ to derive a generalized equation for the cluster operator S:

$$[S, H_0] = (V\Omega - \Omega V_{\text{eff}} + \chi^\dagger(V\Omega - \Omega V_{\text{eff}})_+)_{\text{conn}}$$

where the subscript "+" denotes effects beyond the approximation used. E.g. if singles and doubles are included, only the terms in $(V\Omega - \Omega V_{\text{eff}})_+$ leading to triple or higher excitations are kept. Alternatively, variational principles might be used to derive unitary coupled-cluster equations. This approach was used e.g. by Kutzelnigg [95], Pal [98] and by Bartlett and collaborators [96].

[1] This asymmetry is a consequence of the choice of intermediate normalization. Replacing $\langle c|$ by $\langle c+\delta c|$ would lead to inclusion e.g. of the diagram in Fig. 7e already in the evaluation of the potential from the core

In their most recent calculations on Cs [32, 83] Blundell et al. have added the "Hermitian conjugate" terms leading to the equation:

$$[S_1, H_0] = (V(1+S) - SPVS + S_2^\dagger (VS_2)_3)_{\text{conn},1}$$

for single excitations, while the two-particle equation is unchanged except for the changes induced by the modified S_1.

Liu and Kelly [99] are currently implementing a computer program which includes the VS_2^2 terms as well as the Hermitian conjugate terms in the S_1 equation, thus solving the equation:

$$[S, H_0] = (V(1 + S + \tfrac{1}{2}S_2^2) + S_2^\dagger (VS_2)_+ - SPVS)_{\text{conn}}. \tag{25}$$

The restriction to double excitation clusters S_2 in some of the terms in this equation follows from a restriction to terms which enter in third order of the Coulomb interaction or lower.

3.3. Coupled-cluster equations and additional perturbations

A natural extension of the coupled-cluster approach in the presence of an additional perturbation is to obtain cluster operators which include the perturbation. This extension was suggested by Monkhorst [100] as a method to derive algebraic equations for "first-order properties", with the possibility to compute also second- and higher-order properties. One way is to obtain, e.g., parity mixed-cluster operators, S^{PNC} would be to let all orbitals be parity mixed (i.e. solutions to Eqs. (12–13) and keeping terms with one occurrence of a PNC interaction. Alternatively a closely related double perturbation approach may be used, as in the early work of Kelly [101], where one electron-electron interaction is replaced by the additional perturbation. The relation between the perturbed coupled-cluster expansions based on these two approaches has been discussed e.g. by Bartlett [102].

Liu and Kelly [99] are using a double-perturbation approach. As the PNC operator leads to single excitations already in lowest order, S_1^{PNC} terms must be kept in some cases where the unperturbed cluster Eqs. (25) were restricted to two-particle clusters. Again, keeping terms up to third order in the Coulomb in Coulomb interaction gives

$$[S^{\text{PNC}}, H_0] = H^{\text{PNC}}(1 + S + S_1 S_2)$$
$$+ (V(S^{\text{PNC}} + S^{\text{PNC}} S) - S^{\text{PNC}} PVS + (S_2^{\text{PNC}})^\dagger (VS_2)_3 + S_2^\dagger (VS_2^{\text{PNC}})_3)_{\text{conn}}.$$

These PNC mixed cluster operators can then be used to evaluate the matrix elements of the dipole operator.

An alternative path, followed by Blundell et al. [32] is to use the unperturbed cluster operators for the initial and final states, as well as for the most important intermediate states, to evaluate matrix elements both of the PNC weak interaction and of the dipole operator. These calculations will be discussed in more detail below.

3.3.1. Matrix elements in the coupled-cluster approach. Matrix elements of an additional perturbation can be treated in a number of ways. Formally, the most natural extension of the unperturbed coupled-cluster approach is to introduce perturbed coupled-cluster operators, as discussed above. In the case of a (pseudo-)scalar operator, such as the PNC weak interaction, this is feasible. For

a vector property, such as the external electric field, this leads to an order-of-magnitude increase in the number of angular momentum structures of a pair excitation and due to the size of the problem, this approach does not appear to be very attractive. In addition, unless the coupled-cluster formalism used is unitary, this leads to a different treatment of initial and final states, which is, at least, an aesthetical disadvantage.

A direct evaluation of the matrix element between coupled-cluster wavefunctions, as suggested e.g. in early work by Čížek [87] and by Fink [103], is automatically symmetric in initial and final state. On the other hand, this approach has the disadvantage that the series of diagrams never terminates, although certain types can be summed by a simple matrix inversion and others by iterative schemes [90]. Still, if the coupled-cluster wavefunctions are obtained in a non-Hermitian framework, some simple diagrams are left out already in third order of the electron-electron interaction – unless triple excitations are allowed. In view of the size of the problem it is desirable to avoid triple excitations whenever possible and to include as many terms as possible within the CCSD approach. As a final consideration we mention the fact that the initial and final states of the transition often have the same angular symmetry and should preferably be treated within the same model space. The formalism must thus be able to handle a multiconfigurational, non-degenerate model space. It is possible that a bivariational approach, such as the "Extended coupled-cluster method" (ECCM) suggested by Arponen et al. [104] may have the desired features, but the details involved in an atomic physics implementation have not yet been considered.

Blundell et al. [32, 82–83] restrict the wave operator to linear terms, $\Psi = (1 + S)\Psi_0$ leading to an automatic truncation in the expansion of the matrix elements. In addition, the resulting expression for the matrix element was extended to incorporate the RPA terms exactly. This formalism was found to reproduce the experimental s and $p_{1/2}$ state hyperfine constants with about 1% accuracy. (The experimental valence removal energies were reproduced to about 0.5% or better (about 5% of the total correlation effect) by the solution of Eq. (24).) The technique was then used to evaluate the individual matrix elements $\langle X|H^{\mathrm{PNC}}|I\rangle$, $\langle F|H^{\mathrm{PNC}}|X\rangle$, $\langle X|D|I\rangle$ and $\langle F|D|X\rangle$ for the first four excited $P_{1/2}$ states in X in Eq. (5). The effect of the remaining $P_{1/2}$ states were estimated using the simpler methods presented in Sects. 2.7 and 3.1.

3.4. The need for triple excitations

The Hermitian form of the coupled-cluster expansion leads to inclusion of some terms (e.g. Fig. 7c–e) which are classified as triple excitations in the more conventional approaches based on an intermediate normalization. However, the high demands for accuracy in the PNC calculations will probably necessitate the inclusion also of genuine triple excitations, examples of which are shown in Fig. 8. Salomonson and Ynnerman [91] investigated selected triples diagram contributing to the binding energy and hyperfine structure for Na and found a significant improvement in the agreement with experiment. Complete single, double and triple excitation coupled-cluster procedures (CCSDT) have been implemented by Bartlett and coworkers [104] and by Scuseria and Schaefer [106] and applied to small atomic and molecular systems, using relatively small analytical basis sets. In addition, several methods which include triples in

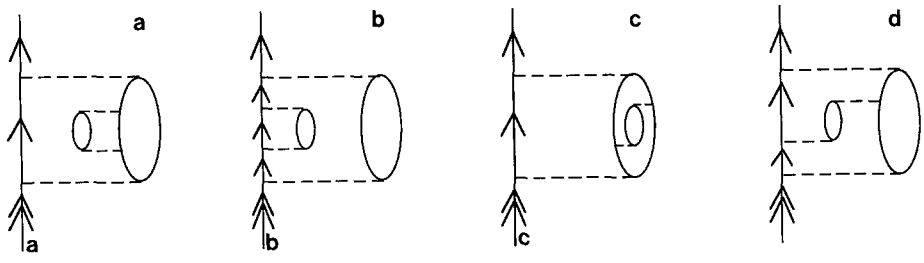

Fig. 8a–d. Examples of triple excitation contributions to a Brueckner orbital

approximate ways have been proposed and tested [105]. Comparisons between the various methods [107, 108] show that the triples contributions from a CCSDT calculation are generally well reproduced by using CCSD amplitudes to evaluate the triples contributions only to lowest order. This observation is encouraging and may make it possible to perform similar calculations for Cs.

3.5. Refined semi-empirical calculations

During the last few years a number of refined semi-empirical methods have been devised, making it possible to combine the stringency of MBPT with the benefits of using accurate experimental data if available.

3.5.1. Direct use of experimental energies and matrix elements. In 1986 Bouchiat and Piketty [26] pointed out that for the $6s \rightarrow 7s$ transition in Cs, the summation in Eq. (5) is strongly dominated by the lowest intermediate p states: $6p$, $7p$ and $8p$ contribute about 95%. If accurate experimental data are available for the energies and relevant matrix elements involving the first few intermediate states, these data can then be used to obtain high accuracy in the dominating part of the result. Two possible problems may be identified: First, the remaining parts of the calculation must be performed in a way consistent with the use of empirical matrix elements. This problem, discussed in more detail below, has been addressed particularly in two recent papers by Hartley and Sandars [29–30]. Second, while the energies and electric dipole transition matrix elements can be deduced directly from experiment, this is not the case for the matrix element of the PNC interaction. However, in the central-field model (CFM) the PNC matrix elements can be obtained from the geometrical mean of the hyperfine structure for the s and $p_{1/2}$ states involved, and Bouchiat and Piketty [26] argue that the ratio between these two properties should be less sensitive to calculational errors than either separately. We note first that the CFM ratio is unchanged by the inclusion of the "external" correlation effects, such as those shown in Fig. 6a–c but also higher order contributions of similar type, since their effect, both on the hyperfine interaction and on the PNC matrix elements is described by the change in wavefunction normalization close to the nucleus. The "core polarization" effects (Fig. 2), on the other hand, will affect the two properties differently, one being a pseudoscalar, the other a vector. Bouchiat and Piketty [26] calculated the lowest order core-polarization contributions for the two properties, which was found to give about 4–5% correction to the ratio (which can be compared to nearly 20% correction for the PNC matrix element, itself [22]). At this stage, the

calculations omit second- and higher-order core-polarization corrections to the ratio, as well as the combined effect of electric dipole shielding and PNC core polarization (e.g. Fig. 4d–e). Internal substitution, such as Fig. 6, are also omitted, but as discussed earlier, these effects are very small for Cs. Their final result quoted is $-0.935(1 \pm 0.02(\text{exp}) \pm 0.03(\text{theory})) \times 10^{-11} i|e|a_0 Q_W/(-N)$.

3.5.2. Correlation potentials. Experimental data can also be used to parameterize a semi-empirical correlation potential to be added to the DHF potential. This approach has been pursued by two groups. Parpia et al. [31] used the experimental polarizability and varied the "cut-off" parameter in the correlation potential. They calculated the shielding effects only approximately, by using a semi-empirically modified dipole operator. As they calculated no other physical quantities, the accuracy of their final result is difficult to assess. Hartley and Sandars [29] chose instead to vary two parameters, namely the overall size of the potential and the "cut-off" parameter, to optimize the energy eigenvalues for the lowest s and p states. Since the additional semi-empirical potential term is intended to account partly for the "external" correlation effects which were not calculated explicitly, it is not removed in the perturbation expansion. This makes possible a consistent treatment of all core polarization effects to higher orders, using the standard RPA equations (12–17), while including the dominating correlation effects via the semi-empirical potential.

Parameters in the correction potential chosen to fit the energies were found to lead also to excellent E1 transition matrix elements, which could be explained by the observation that, the fittting of the eigenvalues leads to an accurate reproduction of the form of the wavefunction for larger r values, which are important for the electric dipole matrix element [29]. On the other hand, the hyperfine values for the s states were overestimated in this approach whereas for the $p_{1/2}$ states they were underestimated, with errors in the range 4–8% of the experimental values. The PNC matrix elements, however, which involve a product of the s and $p_{1/2}$ wavefunction, are much more stable and Hartley and Sandars found a spread of about 1% in their final PNC-E1 matrix elements.

3.5.3. The Semi-Empirical Ratio method. After an analysis of the semi-empirical approach in MBPT terms Hartley and Sandars [30] devised a method to improve calculated PNC-E1 matrix element through careful comparison of calculated results for known quantities with experimental data. They first consider the application of perturbation theory to the ratio between the geometrical mean of the s and $p_{1/2}$ hyperfine structures and of the PNC matrix element. When these matrix elements are evaluated between physical states, the PNC potetnial correction in Fig. 2 and Eqs. (12–13) will involve the energy difference between the two participating states, analogous to the treatment of the time-dependent perturbation in Eqs. (14–15). This difference in the PNC potential corrections arises because the energy denominators involved are always evaluated *towards* the PNC interaction, from above in Fig. 2(c) and from below in Fig. 2(b). (In practice, the presence of ω of the denominators was found to affect the results only in the fourth digit for Cs.) It is then important that the calculation of the residual terms is made in a way consistent with this treatment – which is not the standard computational form. Hartley and Sandars [30] found that it was possible to account for this inconsistency by adding and subtracting the contributions from the low-lying states, as calculated in the more standard formulation and obtain a correction term which is the difference between empirical and calculated contributions from the low-lying states. This correction, which is to be

added to the total calculated result, is expressed as a correction factor multiplying the calculated value for each of the low-lying intermediate states. This type of correction can, of course, be applied for any choice of computational method used and the accuracy of the final result will depend both on the accuracy of the calculation for the higher intermediate states and on the accuracy of the experimental quantities used to obtain the correction factors for the lower ones. The error in E_1^{PNC} due to experimental uncertainties was found to be about 1.5%. The uncertainty entering through the remaining terms is reduced by the smallness of the results for these correction terms found in other works. Accounting for these terms, as well as for the computational uncertainty, Hartley and Sandars obtain a final result $-0.904(1 \pm 0.02) \times 10^{-11}(i|e|a_0 Q_W/-N)$.

4. Results and discussion

Already in Sect. 2 we presented some of the first semi-empirical estimates. The last decade has seen a rapid development of techniques and computers, making possible extensive many-body calculations. Results obtained at various levels of approximation are shown in Table 1. It is hoped that this Table should make it easier for possible newcomers in the field to find relevant numbers for comparison.

The number quoted for the PNC electric dipole transition matrix element is traditionally $\langle 7s^{\mathrm{PM}}(m=1/2)|\boldsymbol{D}|6s^{\mathrm{PM}}(m=1/2)\rangle$ where the superscript PM denotes parity-mixed states. Further, the experimental results assume that the dipole operator is defined as $\boldsymbol{D} = \sum_i |e|\boldsymbol{r}_i$ and here we follow this convention. (The sign choice in $\boldsymbol{D}$ determines the sign of E_1^{PNC}, but leaves the vector Stark polarizability β unchanged, thereby determining the sign of the ratio E_1^{PNC}/β.)

4.1. Results of many-body calculations

The first many-body calculation for Cs was published by Dzuba et al. [20]. The starting point for the calculation was the Dirac–Hartree–Fock potential from the closed-shell core of Cs^+. Correlation effects were taken into account by defining a correlation potential $\Sigma(\varepsilon)$ with the energy ε, which enters the denominator in (20), chosen to be ε_{6s} for all ns states, $\varepsilon_{6p_{1/2}}$ for all $np_{1/2}$ states, etc. This potential was treated to all orders for all intermediate states with one electron outside closed shells, and was found to give energies for 6–8s and 6–8p within 1% of the experimental values. For intermediate states involving core excitations, the correlation potential was neglected. Potential corrections from h^{PNC} were treated self-consistently, whereas the shielding of the electric field was included to lowest order only. Neglecting correlation effects gave the value $-0.880 \times 10^{-11} i|e|a_0(Q_W/-N)$, which was changed to $-0.856 \times 10^{-11} i|e|a_0(Q_W/-N)$ by the inclusion of the correction potential. The velocity form of the dipole operator was found to be much more unstable. Since the shielding of the electric field was not treated self-consistently, the final result may differ between the length and velocity form, and the difference may be used as an indication of the accuracy of the calculation. The discrepancy was found to be significantly reduced by inclusion of the correlation potential: In the DHF basis, the velocity form gave a result 20% lower than that obtained for the length form, whereas in the correlated basis, it was only 0.2% lower. Using

Table 1. Contributions to the $6s \rightarrow 7s$ parity non-conserving electric dipole transition element in Cs due to the spin-independent weak interaction (Eq. (1)) in units of $-10^{-11} \times i|e|a_0 Q_W/(-N)$

	0:th order (Fig. 1)	$+v^{\mathrm{PNC}}$ (Fig. 2)	$+v^{\pm}$ (Fig. 3)	$+v^{\pm\mathrm{PNC}}$ (Fig. 4)		
Local	1.33[a]					
	1.15[b]					
	1.00[c]					
	1.05[d]		0.97[d]			
Dirac–Fock	0.740[e]	0.920[e]		0.880[e]		
	0.736[f]	0.924[f]	0.888[f]	0.886[f]		
		0.92[g]				
		0.912[h]		0.890[i]		
	0.742[j]	0.922[j]		0.887[j]		
				0.866[k]		
		0.927[l]		0.891[l]		
				0.890[m]		
MCDF				0.85[n]		
Brueckner orbitals					Other corrections	Final result
2:nd order				0.904[j]	0.003[j,o,p]	
					−0.003[j,q]	
				0.948[o,r]		
				0.947[k,r]		
		0.983[s]		0.946[s,r]		
				0.929[k,t]		
				0.933[s,t]		
semi-emp.			0.935[u]			
			0.879[v]			
		0.938[l]		0.889[l]		
(+ratio corr)				0.904[x]		0.904(1 ± 0.02)[x]
iterated Σ	0.734[e]	0.907[e]		0.856[e]		
				0.908[k]		
				0.904(6)[m]	−0.001(5)[m,y]	0.903(9)[m]
screened Coul. int.						0.91(1 ± 0.01)[k]
"all-order"				0.911(6)[m]	−0.002[m,z]	0.909(9)[m]

[a] Bouchiat and Bouchiat, Refs. [5, 58]; [b] Loving and Sandars, Ref. [59]; [c] Neuffer and Commins, Ref. [65]; [d] C. Bouchiat et al., Ref. [44] (The smaller number includes semi-empirical shielding effects but no v^{PNC} corrections); [e] Dzuba et al., Ref. [20]; [f] Mårtensson-Pendrill, Ref. [22]; [g] Schäfer et al., Ref. [25]; [h] Johnson et al., Ref. [23]; [i] Johnson et al., Ref. [24]; [j] Dzuba et al., Ref. [13]; [k] Dzuba et al., Ref. [28]; [l] Hartley, Sandars et al., Ref. [29]; [m] Blundell et al., Ref. [32]. The "all order" result includes by construction the internal PNC correlations as well as the "structural radiation" and normalization terms; [n] Plummer and Grant, Ref. [21] (The number quoted in the original work was a factor $\sqrt{(2/3)}$ smaller due to different conventions used); [o] Johnson et al., Ref. [27]; [p] Corrections from Σ^{PNC}; [q] Structural radiation and normalization corrections; [r] Shielding corrections evaluated with DHF orbitals; [s] Hartley et al., Ref. [14]; [t] Shielding corrections evaluated with Brueckner orbitals; [u] Bouchiat and Piketty, Ref. [26]; [v] Parpia et al., Ref. [31]; [x] Hartley and Sandars, Ref. [30]; [y] Internal substitutions, structural radiation, normalization and Breit corrections, to be added to the "iterated Σ" result; [z] Breit interaction

experimental energies, hyperfine splittings and electric dipole transition matrix elements, Dzuba et al. [20] found that their calculated value for the quantity $(A_{7s}A_{6p_{1/2}})^{1/2}\langle 6p_{1/2}|\boldsymbol{d}|6s\rangle(E_{7s}-E_{6p_{1/2}})^{-1}$, which is similar to the PNC-E1 matrix element, was 3.5% too low for the length form (and 0% for the velocity form). Based on this comparison, they quote a final result $-(0.88\pm 0.03)\times 10^{-11}i|e|a_0(Q_W/-N)$ which is 3% higher than their calculated value, but with a 3% uncertainty assigned to it.

A self-consistent treatment of the shielding of the external electric field, as well as the potential corrections due to h^{PNC} (Eqs. 12–17), first developed for calculations on Bi [9] was applied to Cs by Mårtensson-Pendrill [22] giving an automatic identity between the length and velocity form for the dipole operator. The self-consistent treatment of the electric field gives very small contributions for Cs, and the final result is close to the value obtained by Dzuba et al. [20]. The self-consistent treatment of all one-particle effects is now a standard procedure [13, 17, 24, 29]. The small difference seen in Table 1 between the results using this procedure is of the level of sensitivity to the nuclear distribution $\varrho_N(r)$ in h^{PNC} found by Johnson et al. [23]. As discussed in Sect. 3.5.2 Hartley and Sandars have complemented the self-consistent treatment of one-particle effects by adding a correlation potential, thereby obtaining overall better agreement with experimental quantities, where available.

Also the calculations of lowest-order correlation effects has now been performed by several groups [13–14, 27–28]. The disagreement between the first two published results at this level [13, 17] has since been resolved and understood in terms of an insufficiently large basis set used in Ref. [13]. The present results now give a mutual confirmation of the numerical reliability of the second-order Brueckner orbital value $-0.93\times 10^{-11}i|e|a_0(Q_W/-N)$ (with all screening effects evaluated with Brueckner orbitals).

However, as discussed in Sect. 3.1.1, higher-order correlation effects are necessary for the results to be also physically accurate. Adding a semi-empirical correlation potential [29] accounts to some extent also for higher-order correlation effects, in such a way as to reproduce experimental energies, and gives $-0.889\times 10^{-11}i|e|a_0(Q_W/-N)$. The semi-empirical ratio corrections [30], discussed in Sect. 3.5.3, changes this value to $-0.904\times 10^{-11}i|e|a_0(Q_W/-N)$.

Iteration of the correlation potential using Eq. (23) has been found to reduce the result significantly, and Blundell et al. [32] obtain the result $-0.904(6)10^{-11}i|e|a_0(Q_W/-N)$ with an additional correction $+0.001(5)\times 10^{-11}i|e|a_0(Q_W/-N)$ due to internal substitutions, structural radiation and normalization corrections, as well as the modification caused by the Breit interaction. (The error in the correction is due mainly to the estimate of the structural radiation terms.)

By coincidence, a similar value results when the screening of the electron-electron interaction is included, as discussed by Dzuba et al. [28, 76–77]. Blundell et al. [32] investigate the influence of this effect by multiplying the correlation potential Σ by a screening factor λ, where $\lambda=0.8$ for s states and $\lambda=0.84$ for $p_{1/2}$ states were chosen to fit experimental energy levels. This changed the prediction for E_1^{PNC} by only a few tenths of a percent.

The most complete calculation to date [32] includes pair correlation effects to all orders for the matrix element involving the first four excited $P_{1/2}$ states, with effects of the remaining $P_{1/2}$ states, both those involving excitations of the valence electrons and those involving also excitations of core electrons, estimated using the simpler methods presented in Sects. 2.6 and 3.1. These residual

contributions were found to contribute only about 2% of the total E_1^{PNC}. To gain some idea of the accuracy of this calculation, Blundell et al. [32] made various tests:

(a) the coefficients for valence single excitations were rescaled to reproduce the experimental valence removal energy,

(b) a similar modification was made to fit instead the hyperfine constants and

(c) the effect of using the dipole operator in both its length and velocity form was considered

(d) experimentally available energies and oscillator strengths were used where available.

The resultant scatter in the values of E_1^{PNC} was used to estimate a theoretical error of 1%. The vector Stark polarizability for $6s \rightarrow 7s$ transition was also calculated using an analogous technique (see Sect. 4.2, below).
The result $-0.909(9) \times 10^{-11} i|e|a_0(Q_W/-N)$ from this calculation is in good agreement with that obtained by the significantly different approach described in Sects. 2.6 and 3.1, (including the "chaining" of the correlation potential Σ, discussed in Sect. 3.1.1) and Blundell et al. [32] quote the final result as the average of the two approaches, giving:

$$-0.906(9) \times 10^{-11} i|e|a_0(Q_W/-N). \tag{26}$$

The result agrees with the final result given by Dzuba et al. [28] who also claim an accuracy of about 1%.

4.2. The vector Stark polarizability

The experiments studying PNC in atomic Cs measure the ratio of the matrix elements E_1^{PNC}/β, where β is the vector Stark polarizability for the $6s \rightarrow 7s$ transition given by [5, 58]:

$$\beta = \tfrac{1}{6} \sum_n \langle 7s \| \boldsymbol{D} \| nP_{1/2} \rangle \langle nP_{1/2} \| \boldsymbol{D} \| 6s \rangle \left(\frac{1}{E_{7s} - E_{np_{1/2}}} - \frac{1}{E_{6s} - E_{np_{1/2}}} \right)$$
$$+ \tfrac{1}{2} \langle 7s \| \boldsymbol{D} \| nP_{3/2} \rangle \langle nP_{3/2} \| \boldsymbol{D} \| 6s \rangle \left(\frac{1}{E_{7s} - E_{np_{3/2}}} - \frac{1}{E_{6s} - E_{np_{3/2}}} \right). \tag{27}$$

Owing to the availability of experimentally derived values for the $n = 6, 7$ dipole matrix elements and the rapid convergence of the sum over n, semi-empirical estimates of β have been very successful. Typically, the oscillator strengths $f(6s \rightarrow 6p)$ and $f(6s \rightarrow 7p)$ are taken from a direct measurement, while those for $7s \rightarrow 6p$ and $7s \rightarrow 7p$ are inferred from the $7s$ lifetime and the $7s$ polarizability. In one approach, a related quantity α, the scalar transition polarizability, is first calculated and β is then obtained from a measurement of α/β. The calculation of α involves experimental dipole matrix elements and energies for $n = 6, 7$ (in a formula analogous to (27), above), and a theoretical determination of the contribution from $n = 8$ onwards (see e.g. Ref. [109] and further references therein). Recent determinations along these lines give $\beta = 27.2(4) a_0^3$ [26] and $\beta = 27.3(4) a_0^3$ [109]. Recently, Bouchiat and Guena [110] have proposed inferring β from a measurement of M_1^{hfs}/β, where M_1^{hfs} is the component of the

$6s \rightarrow 7s$ magnetic dipole amplitude induced via the hyperfine interaction with the nucleus. Using a theoretical value for M_1^{hfs} they obtain $\beta = 27.17(35)a_0^3$. Thus semiempirical approaches to β already attain the 1.5% level of accuracy. Recently Blundell et al. [32] have published an ab initio calculation using a method analogous to that for E_1^{PNC} described in Sect. 3.3, obtaining $\beta = 27.00(20)a_0^3$. It seems that future progress could result from a combination of improved measurements and more refined calculations.

4.3. *Comparison with experiment*

We are now in a position to extract information from a high-accuracy measurement of caesium PNC. The most accurate experiment [18] reports

$$\mathrm{Im}(E_{\mathrm{PNC}})/\beta = \begin{cases} -1.513(50)\ \mathrm{mV/cm}(F = 3 \rightarrow F' = 4) \\ -1.639(48)\ \mathrm{mV/cm}(F = 4 \rightarrow F' = 3) \end{cases} \tag{28}$$

After estimates of the contributions from the nuclear-spin dependent PNC effects (Eqs. (2)–(3)), discussed in more detail in Refs. [32, 42–43], a value for the spin-independent part of E_1^{PNC} can be extracted, giving $\mathrm{Im}(E_1^{\mathrm{PNC}})/\beta = -1.572(35)$ mV/cm. Using the value $\beta = 27.00(20)a_0^3$ obtained by Blundell et al. [32] and converting the experimental result to atomic units gives

$$E_1^{\mathrm{PNC}}(\mathrm{exp}) = -0.8252(184)[61]10^{-11} ie a_0 \tag{29}$$

where the first error is due to experiment and the second, in square brackets, is the theoretical error from the calculation of β. Combining this value with the calculated value in (26), we can finally determine Q_W as

$$Q_W = -71.04(1.58)[0.88] \tag{30}$$

where two theoretical errors have been taken in quadrature.

4.4. *Particle physics implications*

One of the prime motivations for introduction of the unified theories of weak and electromagnetic interactions was the need for a finite theory. Although the original four-fermion interaction provided a satisfactory tree-level account of weak interaction physics, uncontrollable ultraviolet infinities resulted when radiative corrections were considered. While these could be made somewhat less severe by introducing intermediate charged vector bosons, W, they were completely controlled only when the Z boson and the photon were introduced in $SU(2) \times U(1)$ gauge group with their masses generated by the Higgs mechanism [37]. Once this renormalizable theory was introduced, one loop corrections to weak processes could be unambiguously calculated. Since the coupling constants g and g' of the standard model are proportional to the electric charge e, radiative corrections are proportional to the fine structure constant α, and thus can be expected to enter at the 1% level. In fact, the large mass scale set by the W and Z masses leads to logarithms with large arguments that make these corrections enter at the several percent level. Because, as argued in this paper, the precision of atomic calculations in caesium is at the 1% level, once experiment reaches this level, information about the radiative corrections can be obtained. This is of particular interest since these corrections provide an indirect probe of physics at

a very high energy scale, that normally is probed only with extremely large scale accelerators. The point is that while heavy, undiscovered particles can be directly discovered at such machines, because they enter as virtual particles in radiative corrections, their effect can actually be seen if high-precision low-energy experiments such as atomic parity non-conservation are carried out. A particularly important example of this involves the so-far undiscovered top quark t. From considerations involving the mass of the W, the mass of this particle is known to be around 140 GeV, with an uncertainty of ± 40 GeV. Any variation from the central value can be parameterized in terms of a quantity ϱ multiplying Q_W

$$\varrho_{\text{new}} = 1 + \alpha(m_Z)T$$

where

$$T = \frac{3}{16\pi x_0}\left(\frac{m_t^2 - (140\ \text{GeV})^2}{m_W^2}\right)$$

with $\alpha(m_Z) \approx 1/128$ and $x_0 = 0.2323$ is the value of the square of the sine of the Weinberg angle inferred from the Z mass when $m_t = 140$ GeV. Note that the fine structure constant, α, is normally 1/137, but radiative corrections change it to the value $\alpha(m_Z)$ at the Z mass scale. Using $m_W = 80$ GeV, one can see that the corrections to ϱ can be as large as 2% for $m_t = 200$ GeV. A recent development in the field has been a parameterization of new physics entering radiative corrections by Peskin and Takeuchi [111], which has been extended by Marciano and Rosner [112] to the atomic physics case. In that work a quantity analogous to T called S has been introduced, where S parameterizes the effect of new particles entering vacuum polarization loops in a weak isosopin conserving manner, while T parameterizes weak isosopin breaking effects. This new parameter S is sensitive to new physics at the TeV scale, and in particular is quite large, about 2, for technicolour theories [113]. As an example of this parameterization, one can show, following Ref. [112], that the W mass, which has been measured to be (80.14 ± 0.31) GeV, obeys:

$$m_W = (80.20 - 0.29S + 0.45T)\ \text{GeV}.$$

With the neglect of S, one can see that this provides an upper bound to the top quark mass, but with the inclusion of S one can only bound a range of S and T. However, when the same analysis is applied to atomic physics, one finds for the radiatively corrected weak charge.

$$Q_W = -(73.20 \pm 0.13 - 0.8S - 0.005T).$$

The remarkable feature of this equation is that the T dependence is almost completely negligible. This follows from a cancellation of the T dependence of the overall scaling factor ϱ_{new} with an opposite dependence on T in the square of the sine of the Weinberg angle. The result is that even without a precise determination of the top quark mass, atomic PNC gives an unambiguous prediction sensitive only to the new physics in S. The insensitivity of atomic PNC results to the top quark mass was found also in a somewhat different analysis by Sandars [114]. He made use of the fact that the Z boson mass is now well-known experimentally and formed the product $G_F Q_W M_Z^2$ which he found to be essentially insensitive to $\sin^2\theta_W$ for plausible values. In fact, this product has a minimum with respect to variations in $\sin^2\theta_W$ for a ratio N/Z close to that for heavy atoms. At this point one sees that technicolour theories are in some trouble, since they lead to a value of -74.8 for the weak charge Q_W, which is

known from atomic physics experiments to be $-71.04 \pm 58 \pm 0.88$. This discrepancy of more then 2 experimental standard deviations from the prediction of technicolour theories is at present the most serious challenge to such theories. The only other electroweak experiment equally sensitive to S involves measuring asymmetries in the decay of the Z, and while important to pursue, is at present not of high accuracy.

There is one other way new particle physics can influence atomic PNC. This is any tree-level process involving new Z's, that in general couple to quarks and leptons differently from the Z. Because the standard model is quite successful, these new Z's are in general quite heavy: an illustrative example from an $SO(10)$ model [115] has a Z_χ boson which changes Q_W by $\Delta Q_W = 84 m_W^2 / m_{Z_\chi}^2$. A value of about 500 GeV for the mass of this particle could explain the discrepancy discussed above if the experimental value does not change. As with S, atomic PNC is particularly sensitive to this kind of new physics compared with other particle physics experiments. However, it is important to stress that in order to sort out possible new physics, all electroweak experiments should be pushed to the highest accuracy possible. The main point of this paper is that atomic theory has advanced to a point where the caesium experiment can play an important role in this process.

5. Conclusion and outlook

We have seen that atomic physics experiments provide valuable complements to high-energy physics experiments in the study of weak interaction. Future experimental developments are expected to lead to increased accuracy for Cs, as well as for the other heavy atoms, Tl, Pb and Bi, for which PNC effects are studied. This will push atomic theory to its limits – we can note that the inclusion of thousands of pair excitations, as in the recent Cs calculation [32], with 20–25 basis function used to express each orbital symmetry, corresponds to several million configurations. To reach an accuracy of 0.1%, which would be desirable in the not too distant future, requires the inclusion of triple excitations, clearly would be even more demanding.

In view of the significance of the results, it is important that as many different methods as possible are applied to the calculations. So far, the extensive machinery developed by quantum chemists has not been applied to this problem. One obstacle on the way is the need for a relativistic treatment. In addition, the contact nature of the weak interaction demands the inclusion of high-energy unperturbed orbitals for the representation of the quite localized orbital corrections – more than one published result has suffered from insufficient basis sets. However, with the rapid developments of computing facilities and progams, we expect these problems to be overcome in the future.

In attempts to circumvent the need for atomic theory, experiments are also underway to study PNC in a sequence of isotopes of an element, such as Sm [116] and Cs [117], following the suggestion by [118]. The motivation for these studies is that the electronic wavefunction is determined mainly by the nuclear charge (and to a small extent by its distribution) and can be expected to be essentially the same for all the isotopes of an element. The dependence on the atomic structure can then be factored out and the results would be proportional to Q_W. However, these experiments may shift the burden to nuclear theorists: the changes in neutron distribution may affect the result at the desired level of accuracy [119], but cannot be obtained directly from experiment, in contrast to

changes in nuclear charge distribution, which may be deduced from optical isotope shift studies.

The increased experimental accuracy may also make possible unambiguous observation of the nuclear spin-dependent terms (cf. Ref. [18]), in particular those caused by a "nuclear anapole moment", discussed in Sect. 2.1. Further, the PNC electron-electron interaction remains to be observed. With its smaller Z enchancement, it is clear that it would be observed only in experiments designed specifically to look for this interaction. Early works suggested experiments helium-like systems [120], as well as on diatomic molecules [121], where PNC effects would be enhanced due to the existence of nearby levels of opposite parity [122–123]. However, no such experiments appear to have been performed.

A more direct need for molecular calculations arises from the careful experiments on TlF [124], searching for effects that violate symmetry under both parity and time reversal. This closely related problem has been studied also in atomic systems and recent reviews on the motivation and requirements for these experiments and calculations have been given elsewhere [125].

With the effect of the weak interaction in atomics systems well established, we may proceed with the speculation that this asymmetry in fundamental interactions may be responsible for the observed handedness in biomolecules (e.g. the famous double helix of the DNA carrying our genetic codes is always right-handed). This was first suggested by Vester and Ulbricht [126] and has recently been discussed e.g. in Ref. [127]. This "mono-chirality" may result from different mechanisms. The weak interaction would lead to slightly different energies between the two forms of a molecule. Theoretical estimates of this effect [128] indicate that it is too small to be responsible for the biomolecular handedness. Another possibility is a different reaction rate for the left- and right-handed forms of a molecule when exposed to polarized electrons, e.g., from the β-decay of ^{14}C, which was present in the early universe. However, the experimental situation is somewhat unclear. Whereas some experiments have found asymmetries [129] others have failed to observe such effects [130] and, where observed, the effects have been much larger than quantitative theoretical predictions [131]. Thus, the answer to our speculative question will have to await further experimental confirmation, as well as development in other fields, such as models for the early universe and evolutionary biology, which are outside the scope of ab initio atomic or molecular calculations.

Acknowledgements. This joint paper is a result of the participation in the workshop on Coupled Cluster Theory at the Interface of Atomic Physics and Quantum Chemistry, Aug. 1990, and we would like to thank the organizers Rodney Barlett and Bhanu Das for a stimulating week in Harvard. Financial support from the National Science Foundation, NSF Grant No PHY-89-07258 (SAB, ZWL and JS), from the British Science and Engineering Research Council, SERC (ACH) and from the Swedish Natural Science Research Council, NFR (A-M M-P) is gratefully acknowledged. Further, ACH and A-M M-P would like to acknowledge a grant from the "Swedish Institute" making possible a collaboration on part of this project. Finally, we would like to express our appreciation of our collaborators in the study of PNC: Walter Johnson, Pat Sandars and Eva Lindroth, who were unable to attend the workshop.

References

1. Purcell EM, Ramsey NF (1950) Phys Rev 78:807
2. Wu CS, Ambler E, Hayward RW, Hoppes DD, Hudson RP (1957) Phys Rev 105:1413

3. Weinberg (1967) Phys Rev Lett 19:1264; (1980) Rev Mod Phys 52:515; A Salam: Svartholm N (ed) in Elementary Particle Theory, Proc. 8th Nobel Symposium. Almquist and Wiksell Förlag, Stockholm 1968; (1980) Rev Mod Phys 52:525; (1961) Glashow SL (1961) Nucl Phys 22:579; (1980) Rev Mod Phys 52:539
4. Hasert FJ (1973) Phys Lett 46B:138
5. Bouchiat MA, Bouchiat C (1974) Phys Lett 48:111; (1974) J Physique (Paris) 35:899
6. See e.g. the article entitled "Why all the fuss about bismuth" by Feinberg G (1979) Comm Nucl Part Phys 80:143
7. See e.g. the review by Fortson EN, Lewis LL (1984) Phys Rep 113:289; and the more recent experimental work by MacPherson MJ, Stacey DN, Baird PEG, Hoare JP, Sandars PGH, Tregidgo KMJ, Guonen Wang (1987) EPS Lett 4:811
8. Harris MJ, Loving CE, Sandars PGH (1978) J Phys B 11:L749
9. Mårtensson AM, Henley EM, Wilets L (1981) Phys Rev A24:308
10. Dzuba VA, Flambaum VV, Silvestrov PG, Sushkov OP (1988) EPS Lett 7:413 includes references to earlier calculations for Bi
11. Drell PS, Commins ED (1984) Phys Rev Lett 53:968; (1985) Phys. Rev. A32:2196; Tanner C, Commins ED (1986) Phys Rev Lett 56:332
12. Das BP, Andriessen J, Vajed-Samii M, Ray SN, Das TP (1982) Phys Rev Lett 49:32
13. Dzuba VA, Flambaum VV, Silvestrov PG, Sushkov OP (1987) Physica Scripta 35:69; (1987) J Phys B21:3297 includes a comprehensive list of references to older PNC calculations for Tl
14. Hartley AC, Lindroth E, Mårtensson-Pendrill A-M (1990) J Phys B23:3417
15. Emmons TP, Reeves JM, Fortson EN (1983) Phys Rev Lett 57:2089
16. Novikov VN, Sushkov OP, Khriplovich IB (1976) Zh. ETF 71:1655 (JETP 44:872) (1976)
17. Botham CP, Blundell SA, Mårtensson-Pendrill A-M, Sandars PGH (1987) Physica Scripta 36:481
18. Noecker MC, Masterson BP, Wieman CE (1988) Phys Rev Lett 61:310-3
19. Bouchiat MA, Guena J, Pottier L (1985) J Physique (Paris) 46:1897; Bouchiat MA, Guena J, Pottier L, Hunter LR (1986) J Physique (Paris) 47:1175, 1709
20. Dzuba VA, Flambaum VV, Silvestrov PG, Sushkov OP (1984) Phys Lett A103:265; (1985) J Phys B18:597
21. Plummer EP, Grant IP (1985) J Phys B18:L315
More details can be found in Plummer EP, D. Phil. Thesis, Oxford (1984 or in Mårtensson-Pendrill A-M (1987) Physica Scripta 36:122
22. Mårtensson-Pendrill A-M (1985) J Physique (Paris) 46:1949
23. Johnson WR, Guo DS, Idrees M, Sapirstein J (1985) Phys Rev A32:2093
24. Johnson WR, Guo DS, Idrees M, Sapirstein J (1986) Phys Rev A34:1043
25. Schäfer A, Müller B, Greiner W (1985) Z Physik A322:539
26. Bouchiat C, Piketty C-A (1986) Europhys Lett 2:511
27. Johnson WR, Blundell S, Liu ZW, Sapirstein J (1988) Phys Rev A37:1395
28. Dzuba VA, Flambaum VV, Sushkov OP (1989) Phys Lett A141:147
29. Hartley AC, Sandars PGH (1990) J Phys B23:1961
30. Hartley AC, Sanders PGH (1990) J Phys B23:2649
31. Parpia FA, Perger WF, Das BP (1988) Phys Rev A37:4034
32. Blundell SA, Johnson WR, Sapirstein J (1990) Phys Rev Lett 65:1411
33. Dunford RW, Lewis RR, Williams WC (1978) Phys Rev A18:2421
34. von Oppen G (1990) Europhys Lett 11:25
35. Langacker P (1989) Phys Rev Lett 53:1920
36. Marciano WJ, Sirlin A (1983) Phys Rev D27:522; Amaldi U, Böhm A, Durkin LS, Langacker P, Mann AK, Marciano WJ, Sirlin A, Williams HH (1987) Phys Rev D36:1385
37. Taylor JC Gauge theories of weak interactions, Cambridge University Press, Cambridge 1976
38. Zel'dovich YaB (1957) Zh. E.T.F. 33:1531; Barkov LM, Khriplovich IB, Zolotorev MS (1989) Comments at Mol Phys 23:189
39. Flambaum VV, Khriplovich IB, Sushkov OP (1984) Phys Lett B146:367
40. Khriplovich IB Private communication at ICAP, Ann Arbor, Michigan 1990
41. This contribution due to the electron-electron interaction is significantly smaller than that found in the work by Schäfer et al. Ref. 25

42. Frantsuzov PA, Khriplovich IB (1988) Z Physik D7:297
43. Kraftmakher AYa (1988) Phys Lett A132:167
44. Bouchiat C, Piketty CA, Pignon D (1983) Nucl Phys B221:68
45. Guena J, as quoted in Ref. 26
46. Brown GE, Ravenhall DG (1951) Proc Roy Soc A208:552
47. Sucher J (1980) Phys Rev A22:348; (1984) Int J Quant Chem 25:3
48. Lindroth E (1987) Physica Scripta 36:485; Thesis, University of Göteborg 1987; (1988) Phys Rev A37:316
49. Lindroth E, Heully J-L, Lindgren I, Mårtensson-Pendrill A-M (1987) J Phys B20:1679
50. Grant IP (1982) Phys Rev A25:1230
51. Goldman SP, Drake GWF (1983) J Phys B16:183
52. Quiney HM, Grant IP, Wilson S (1985) J Phys B18:577, 2805; (1989) J Phys B22:L15; (1990) J Phys B23:L271
53. Johnson WR, Sapirstein J (1986) Phys Rev Lett 57:1126; Blundell SA, Johnson WR, Sapirstein J (1988) Phys Rev A37:307
54. Salomonson S, Öster P (1989) Phys Rev A40:5559, 5548
55. Mittlemann MH (1981) Phys Rev. A24:1167
56. Schwarz WHE, Wallmeier H (1982) Mol Phys 46:1045
57. Kutzelnigg W (1984) Int J Quant Chem 25:107
58. Bouchiat MA, Bouchiat C (1975) J Physique (Paris) 36:493
59. Loving CE, Sandars PGH (1975) J Phys B8:L336
60. Green AES, Sellin DL, Zachor AS (1969) Phys Rev 184:1
61. Sandars PGH (1965) Phys Lett 14:194
62. Sandars PGH (1968) J Phys B (Proc Phys Soc Ser 2) 1:499, 511
63. Sternheimer RM (1950) Phys Rev 80:102: (1951) Phys Rev 84:244; (1952) Phys Rev 86:316
64. Lindgren I, Morrison J Atomic Many-Body Theory. Springer Series in Chemical Physics, Vol 13 (1982), 2nd Ed. 1986
65. Neuffer DV, Commins ED (1977) Phys Rev A16:1760
66. Tiez T (1954) J Chem Phys 22:2094
67. Heully JL, Mårtensson-Pendrill A-M (1983) Physica Scripta 27:291
68. Sandars PGH (1977) J Phys B10:2983
69. Dalgarno A (1962) Adv Phys 11:281
70. Amusia MYa, Cherepkov NA (1975) Case Stud At Phys 5:47; Johnson WR, Lin CD, Cheng KT, Lee CM (1980) Physica Scripta 21:409
71. Dalgarno A, Victor GA, (1966) Proc Roy Soc (London) A291:291
72. Garpman S, Lindgren I, Lindgren J, Morrison J (1976) Z Physik A276:167
73. Lindgren I, Lindgren J, Mårtensson A-M (1976) Z Physik A279:113
74. Hartley AC, Mårtensson-Pendrill A-M (1990) Z Physik D15:309
75. Kelly HP (1963) Phys Rev 131:684
76. Dzuba VA, Flambaum VV, Silvestrov PG, Sushkov OP (1988) Phys Lett A131:461 and in: Mohr P, Johnson W, Sucher J (eds) AIP Conference Proceedings 189 "Relativistic, Quantum Electrodynamic and Weak Interactions", Santa Barbara, Jan-June 1988
77. Dzuba VA, Flambaum VV, Sushkov OP (1989) Phys Lett A140:493; (1989) Phys Lett A142: 373
78. Vajed-Samii M, Ray SN, Das TP, Andriessen J (1979) Phys Rev A20:1787; (1981) Phys Rev A24:1204; Das BP, Andriessen J, Vajed-Samii M, Ray SN, Das TP (1982) Phys Rev Lett 49:32
79. Blundell SA, Johnson WR, Sapirstein J, (1990) Phys Rev A42:3751
80. Mårtensson A-M (1979) J Phys B12:3995
81. Salomonson S, Öster P Numerical Solution of the Coupled-Cluster Singles and Doubles (CCSD) Equations with Applications to Be and Li^-. Phys Rev A (in press)
82. Blundell SA, Johnson WR, Sapirstein J (1989) Phys Rev A40:2233
83. Blundell SA, Johnson WR, Sapirstein J Relativistic All-Order Calculation of Energies and Matrix Elements in Cs, Phys Rev A (to be published)
84. Lindgren I (1988) Nucl Inst Meth B31:102; in: Mukherjee D (ed) Aspects of Many-Body Effects in Molecules and Extended Systems, Lecture Notes in Chemistry, Vol 50. Springer, Berlin Heidelberg New York 1989 and J Phys B (in press)

85. Coester F (1958) Nucl Phys 1:421
86. Coester F, Kummel H (1960) Nucl Phys 17:477
87. Cizek J (1966) J Chem Phys 45:4256; (1969) Adv Chem Phys 14:35
88. Kümmel F Theor Chim Acta 80; Cizek J Theor Chim Acta 80
89. Mårtensson-Pendrill A-M, Alexander SA, Adamowicz L, Oliphant N, Olsen J, Quiney HM, Salomonson S, Sundholm D, Öster P Phys Rev A (in press)
90. Mårtensson-Pendrill A-M, Ynnermann A (1990) Physica Scripta 41:329
91. Salomonson S, Ynnermann A Phys Rev A (in press)
92. Mårtensson-Pendrill A-M, Pendrill LR, Salomonson S, Ynnerman A, Warston H (1990) J Phys B23:1749
93. Paldus J, Takahashi M, Cho RWH (1984) Phys Rev B30:4267
94. Paldus J, Cízek J, Takahashi M (1984) Phys Rev A30:2193
95. Kutzenigg W In: Schaefer III HF (ed) Modern Theoretical Chemistry, Vol 4. Plenum Press, New York, 1977, pp. 129–88 (in particular pp 168–72)
96. Bartlett RJ, Noga J (1988) Chem Phys 150:29; Bartlett RJ, Kucharski SA, Noga J (1989) Chem Phys 155:133
97. Jørgensen E (1975) Mol Phys 29:1137
98. Pal S (1984) Theor Chim Acta 66:207
99. Liu ZW, Kelly HP (work in progress)
100. Monkhorst HJ (1977) Int J Quant Chem S11:421; Dalgaard E, Monkhorst HJ (1983) Phys Rev A28:1217
101. Kelly HP (1969) Adv Chem Phys 14:129; (1969) Phys Rev 182:84
102. Bartlett RJ In: Jørgensen P, Simons J (eds) Geometrical Derivatives of Energy Surfaces and Molecular Properties, pp 35–61. Reidel, 1986
103. Fink M (1974) Nucl Phys A221:163
104. Arponen JS, Bishop RH, Pajannel E (1987) Phys Rev A36:2519, 2539
105. Noga J, Bartlett RJ (1987) J Chem Phys 86:7041; Lee YS, Kucharski SA, Bartlett RJ (1985) 81:5906; Urban M, Noga J, Cole SJ, Bartlett RJ (1985) J Chem Phys (1985) 83:4041
106. Scuseria GE, Schaefer HF, (1982) Chem Phys Lett 152:382
107. see e.g. Urban M, Cernusak I, Kellö V, Noga J, Electron Correlation in Molecules. In: Wilson S (ed) Methods in Computational Chemistry, Vol 1. Plenum, New York 1987
108. Scuseria GE, Lee TJ Comparison of Coupled-Cluster Methods which Include the Effects of Connected Triple Excitations. J Chem Phys (in press); Scuseria GE Theor Chim Acta 80
109. Gilbert SL, Wieman CE (1986) Phys Rev A34:792
110. Bouchiat MA, Guena J (1988) J Physique (Paris) 49:2037
111. Peskin ME, Takeuchi T (1990) Phys Rev Lett 65:964
112. Marciano WJ, Rosner JL University of Chicago, preprint EFE-90-55
113. Weinberg S (1979) Phys Rev D19:1277; L Susskind (1979) Phys Rev D20:2619
114. Sandars PGH (1990) J Phys B23:L655
115. London D, Rosner JL (1986) Phys Rev D34:1530
116. Baird PEG et al., private communication
117. Wieman CE, private communication
118. Dzuba VA, Flambaum VV, Khriplovich IB (1986) Z Physik D1:243
119. Fortson EN, Pang Y, Wilets L (1990) Phys Rev Lett 65:2857
120. Gorschkov VG, Klimchitskaya GL, Labzovskii LN, Melibaev M (1977) Zh. ETF 72:1268; Sov Phys JETP (1977) 45:666
121. Labzovskii LN (1976) Zh E T F 73:1623
122. Sandars PGH (1967) Phys Rev Lett 18:1396
123. Sushkov OP, Flambaum VV (1978) Zh ETF 75:1280; (1978) Sov. Phys. JETP 48:608 Gorschkov VG, Labzovskii LN, Moskalev AN (1978) Zh. ETF 76:414; (1977) Sov Phys JETP 49:209
124. Harrison GS, Sandars PGH, Wright SJ (1969) Phys Rev 22:1263; Hinds EA, Sandars PGH (1980) Phys Rev A21:480; Wilkening DA, Ramsey NF, Larson DJ (1984) Phys Rev A29:425 Schropp D, Cho D, Vold T, Hinds EA (1987) Phys Rev Lett 59:991; Cho D, Sangster K, Hinds EA (1989) Phys Rev Lett 63:2559

125. Sandars PGH (1987) Physica Scripta 36:904; Khriplovich IB Atomic Physics 11 Proc. Eleventh ICAP, 1988, pp 113–132; Mårtensson-Pendrill A-M In: Wilson S (ed) Methods in Computational Chemistry, Vol 6. Plenum, to be published
Hunter LR Science, to be published
126. Vester F, Ulbricht TLD, Krauch H (1959) Naturwissenchaften 46:68
127. Mason SF (1984) Nature 311; Kondepudi DK, Nelson GW (1985) Nature 314:438; Hegstrom RE, Kondepudi DK (1990) Sci Am 262:98
128. Hegstrom RA, Rein DW, Sandars PGH (1980) J Chem Phys 73:2329
Mason SF, Tranter GE (1983) Chem Phys Lett 94:34; (1984) Mol Phys 53:1091
129. Conte E, (1985) Lett Nuovo Cim 44:641; (1987) II Nuovo Cim 9D:497; Garay AS (1968) Nature 219:338
130. e.g. Gidley DW, Rich A, van House JC, Zitzewitz PW (1982) Nature 297:639
131. Garay A, Keszthelyi L, Demeter I, Hrasko P (1974) Chem Phys Lett 23:549; (1974) Nature 250:332; Zel'dovich Ya B, Saakyan DB (1980) JETP 51:1118